NASA CR-168260

National Aeronautics and Space Administration

CREEP FATIGUE OF LOW-COBALT SUPERALLOYS: WASPALOY, PM U 700, AND WROUGHT U 700

September 1, 1983

by

B. N. Leis, R. Rungta, and A. T. Hopper

BATTELLE-COLUMBUS LABORATORIES

Prepared for

National Aeronautics and Space Administration

LEWIS RESEARCH CENTER
Contract No. NAS3-23289

23 1 1 RN/NASA-CR-168260

DISPLAY 23/2/1

84N13265*# ISSUE 4 PAGE 498 CATEGORY 26 RPT#: NASA-CR-168260 NAS 1.26:168260 CNT#: NAS3-23289 83/09/01 61 PAGES UNCLASSIFIED DOCUMENT

UTTL: Creep fatigue of low-cobalt superalloys: Waspalloy, PM U 700 and wrought U 700 TLSP: Final Report

AUTH: A/LEIS, B. N.; B/RUNGTA, R.; C/HOPPER, A. T.

CORP: Battelle Columbus Labs., Ohio. AVAIL.NTIS SAP: HC A04/MF A01

MAJS: /*COBALT ALLOYS/*CRACK INITIATION/*CREEP PROPERTIES/*FATIGUE (MATERIALS)/* HEAT RESISTANT ALLOYS

MINS: / CHEMICAL COMPOSITION/ FATIGUE TESTS/ SPECIMEN GEOMETRY/ TEMPERATURE EFFECTS

ABA: S.L.

ABS: The influence of cobalt content on the high temperature creep fatigue crack initiation resistance of three primary alloys was evaluated. These were Waspalloy, Powder U 700, and Cast U 700, with cobalt contents ranging from 0 up to 17 percent. Waspalloy was studied at 538 C whereas the U 700 was studied at 760 C. Constraints of the program required investigation at a single strain range using diametral strain control. The approach was phenomenological, using standard low cycle fatigue tests involving continuous cycling tension hold cycling, compression hold cycling, and symmetric hold cycling. Cycling in the absence of or between holds was done at 0.5 Hz, whereas holds when introduced lasted 1 minute. The plan

ENTER:

1. Report No.	2. Government Accession No.	3. Recipient's Catalog No.
NASA CR-168260		

4. Title and Subtitle	5. Report Date
Creep Fatigue of Low-Cobalt Superalloys: Waspalloy, PM U 700, and Wrought U 700	September 1, 1983
	6. Performing Organization Code

7. Author(s)	8. Performing Organization Report No.
Brian N. Leis, Ravi Rungta, and Allen T. Hopper	
	10. Work Unit No. G-8030-0001

9. Performing Organization Name and Address	11. Contract or Grant No.
Battelle Columbus Laboratories 505 King Avenue Columbus, Ohio 43201	
	13. Type of Report and Period Covered Final

12. Sponsoring Agency Name and Address	14. Sponsoring Agency Code
NASA Lewis Research Center 21000 Brookpark Rd Cleveland, Ohio 44135	

15. Supplementary Notes

16. Abstract

The work was performed in support of the NASA COSAM program. The objective of this study was to evaluate the influence of cobalt content on the high temperature creep fatigue crack initiation resistance of three primary alloys. These were Waspalloy, Powder U 700, and Cast U 700, with cobalt contents ranging from 0 up to 17 percent. Waspalloy was studied at 538 C whereas the U 700 was studied at 760 C. Constraints of the program required investigation at a single strain range using diametral strain control. The approach was phenomenological, using standard low cycle fatigue tests involving continuous cycling tension hold cycling, compression hold cycling, and symmetric hold cycling. Cycling in the absence of or between holds was done at 0.5 Hz, whereas holds when introduced lasted 1 minute. The plan was to allocate two specimens to the continuous cycling, and one specimen to each of the hold time conditions. Data was taken to document the nature of the cracking process, the deformation response, and the resistance to cyclic loading to the formation of small cracks and to specimen separation. The influence of cobalt content on creep fatigue resistance was not judged to be very significant based on the results generated. However, this situation may be a consequence of the type of experiments performed meaning the conclusions of the study should not be considered as generally valid. Specific conclusions were that the hold time history dependence of the resistance is as significant as the influence of cobalt content and increased cobalt content does not produce increased creep-fatigue resistance on a one-to-one basis.

17. Key Words (Suggested by Author(s))	18. Distribution Statement
cobalt, high temperature creep fatigue crack initiation, Waspalloy, Powder U 700, Cast U 700, deformation response	

19. Security Classif. (of this report)	20. Security Classif. (of this page)	21. No. of Pages	22. Price*
		55	

* For sale by the National Technical Information Service, Springfield, Virginia 22161

NASA-C-168 (Rev. 10-75)

N84-13265#

EXECUTIVE SUMMARY

The objective of this study was to evaluate the influence of cobalt content on the high tempertature creep fatigue crack initiation resistance of three primary alloys. The work was performed in support of the NASA COSAM program. Materials, cobalt contents, and test temperatures investigated were as follows:

Alloy	Cobalt Compositions, %	Test Temperature, C
Waspaloy	13.5, 9.0, 4.5, 0	538
Wrought U 700	17.0, 12.8, 8.6, 4.3, 0	760
Powder MET. U 700	17.0, 12.8, 8.6, 4.3, 0	760

Constraints of the program required investigation at a single strain range using diametral strain control. The approach was phenomenological, using standard low cycle fatigue tests involving continuous cycling tension hold cycling, compression hold cycling, and symmetric hold cycling. Cycling in the absence of or between holds was done at 0.5 Hz, whereas holds when introduced lasted 1 minute. The plan was to allocate two specimens to each of the hold time conditions.

Data was taken to document the nature of the cracking process, the deformation response, and the resistance to cyclic loading. Results were reported for each of the following parameters:

1. Number of cycles to first indication of failure by cracking, N_o.
2. Number of cycles to 10 percent drop in stabilized ratio of peak tensile stress to peak compressive stress, N_i.
3. Number of cycles to 5 percent drop in stabilized load range, N_5.
4. Number of cycles to 50 percent drop in stabilized load range, N_{50}.
5. Number of cycles to failure by complete separation of the specimen, N_f.

6. Total strain range at $N_f/2$.
7. Elastic strain range at $N_f/2$.
8. Inelastic strain range at $N_f/2$.
9. Creep strains per cycle at $N_f/2$.
10. Stress range at $N_f/2$.
11. Amount of stress relaxation per cycle at $N_f/2$.
12. Mean stress at $N_f/2$.

The influence of cobalt content on creep fatigue resistance was not judged to be very significant based on the results generated, and summarized in the following figures.

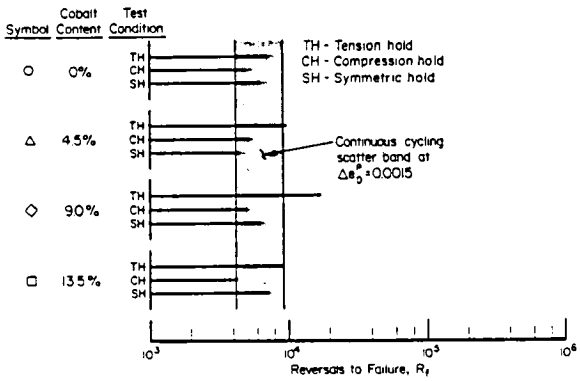

a. for Waspalloy at 538 C at $\Delta e_0^p = 0.0015$

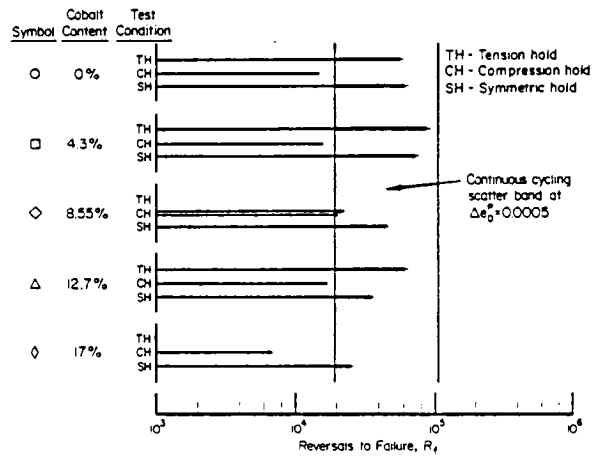

b. for PM U 700 at 760 C at $\Delta e_0^p = 0.0005$

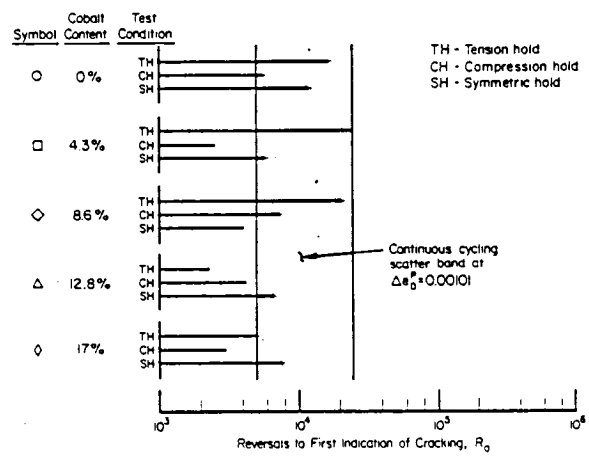

c. for Wrought U 700 at 760 C at $\Delta e_0^p = 0.00101$

These figures show the following:

- the hold time history dependence of the resistance is as significant as the influence of cobalt content and
- increased cobalt content does not produce increased creep-fatigue resistance on a one-to-one basis.

COMPARISON OF FATIGUE RESISTANCES AS A FUNCTION OF COBALT CONTENT AND STRAIN HISTORY AT $\Delta e_0^p = 0.0005$

Throughout the investigation assessing the influence of cobalt content was complicated by the influence of the failure criterion and the method of data presentation and comparison. For example, early on, plastic strain was chosen rather than total strain as the mode for presentation to resolve differences in interpretation. This choice was supported on technical grounds related to the fundamental role of plastic strain in the fatigue damage process. But, the fact remains that total strain is a better criterion at longer lives, so that the choice made may be tenuous in some COSAM applications. Similar confusion might develop if the results were compared in terms of axial versus longitudinal strain, depending on the ratio of $\Delta e_D^P/\Delta e_D^e$. Like problems develop interpreting data for situations where different fractions of N_o/N_f develop over the range of data being compared. This problem was noted as being particularly acute when the significance of cobalt to the crack initiation and growth resistances differs. Again, the choice to use N_o rather than N_f may lead to conclusions that would be inappropriate for certain COSAM applications.

It follows from the above that the eventual application of a material in part controls what cobalt level would be optimal. Given the apparent sensitivity of thermal fatigue and cyclic oxidation resistance to cobalt content, it may be that the best comparitive elevated temperature resistance testing would involve thermal mechanical fatigue (TMF) cycling (perhaps with hold times) in an aggressive environment characteristic of fuel impurities or extreme operation conditions. Such tests, while more difficult to perform, may better define the service significance of cobalt content. But, regardless of the specific test performed, it would be advisable to perform these tests over a broader range of lives. Such studies are relevant in that they would show "crossover" patterns in optimal cobalt contents if the mechanisms controlling intiation and growth change with the increase cycle times. Finally, the viability of predictive methods for creep-fatigue or TMF analysis should be verified. This verification should focus on domains where plastic strains may be small thereby permitting the effect of hold-time induced mean stresses to continue throughout the life of components.

TABLE OF CONTENTS

LIST OF FIGURES

CREEP FATIGUE OF LOW-COBALT SUPERALLOYS: WASPALOY, PM U 700, AND WROUGHT U 700

by

B. N. Leis, R. Rungta, A. T. Hopper, and N. Frey

INTRODUCTION AND OBJECTIVE

This work was performed as a part of a large program whose focus is the conservation of strategic aerospace materials - COSAM. Details of the broad scope and objectives of the COSAM program directed through NASA Lewis Research Center are set forth elsewhere[1]*. Suffice it here to state that the objective of this specific study was to evaluate the influence of cobalt content on the high temperature creep-fatigue crack initiation resistance of three primary alloys. The alloys were Waspaloy, wrought U 700, and powder metallurgy (PM) U 700.

APPROACH AND SCOPE

The approach used was purely phenomenological. Standard low cycle fatigue tests were performed using a minimum test matrix designed to bracket the behavior. Test conditions were guided by the results of eight tests conducted by NASA-Lewis as a preliminary to this study[2]. The three materials were investigated at five cobalt contents and three temperatures. A total of 14 combinations were studied, as set forth in Table 1. All tests for each material were to be conducted under similar test conditions in diametral strain control at a single strain range. The strain range was to be selected to produce lives on the order of 10^4 cycles to separation. Testing was to embrace continuous constant amplitude cycling at 0.5 Hz. Tests were also done using tensile, compressive and symmetric holds of 1 minute introduced into constant amplitude cycling at 0.5 Hz, as schematically depicted in Figure 1.

---

* Numbers in parentheses indicate references on page 51.

TABLE 1. CREEP-FATIGUE OF LOW COBALT SUPERALLOYS

Alloy	Cobalt Compositions, %	Test Temperature, C
Waspaloy	13.5, 9.0, 4.5, 0	538
Wrought U 700	17.0, 12.8, 8.6, 4.3, 0	760
Powder MET. U 700	17.0, 12.8, 8.6, 4.3, 0	760

a. High-Frequency (0.5 Hz) b. Tensile and Comp Creep (1-min each)

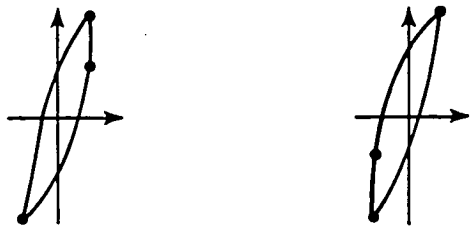

c. Tensile Creep (1-min) d. Comp Creep (1-min)

FIGURE 1. SCHEMATIC OF ANTICIPATED HYSTERESIS BEHAVIOR FOR THE VARIOUS STRAIN-CONTROLLED CREEP-FATIGUE CYCLES

The plan was to commit one specimen to each of these conditions. As noted in Figure 2, which details the testing procedure, a fifth sample was available to duplicate the continuous cycling result or to repeat a questionable test. In all cases this specimen was used to duplicate the continuous cycling test. Testing was done and records were made to generate the following data:

1. Number of cycles to first indication of failure by cracking, N_o.
2. Number of cycles to 10 percent drop in stabilized ratio of peak tensile stress to peak compressive stress, N_i.
3. Number of cycles to 5 percent drop in stabilized load range, N_5.
4. Number of cycles to 50 percent drop in stabilized load range, N_{50}.
5. Number of cycles to failure by complete separation of the specimen, N_f.

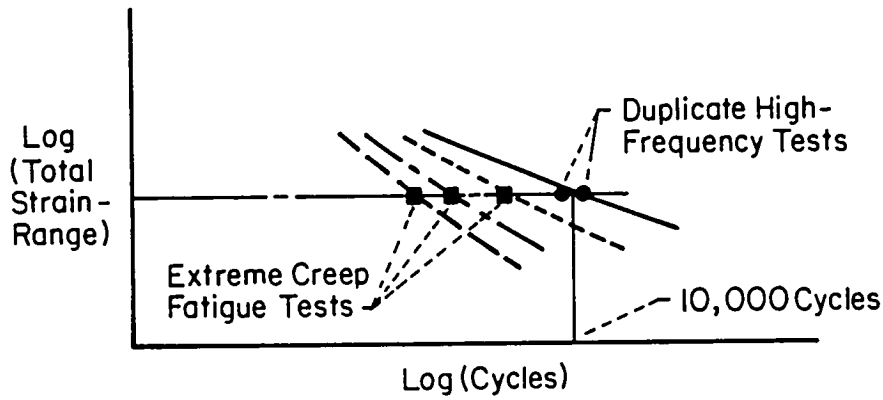

Step 1. Estimate behavior based on tensile and creep properties.

Step 2. Select strain range for $N_f \sim 10{,}000$ high-frequency cycles.

Step 3. Conduct first high-frequency test.

Step 4. Conduct one each of extreme creep-fatigue cycles.

Step 5. Conduct second high-frequency test or repeat questionable tests.

Step 6. Repeat testing sequence for all compositions.

FIGURE 2. EXPERIMENTAL PROCEDURE AND ANTICIPATED RESULTS

6. Total strain range at $N_f/2$.
7. Elastic strain range at $N_f/2$.
8. Inelastic strain range at $N_f/2$.
9. Creep strains per cycle at $N_f/2$.
10. Stress range at $N_f/2$.
11. Amount of stress relaxation per cycle at $N_f/2$.
12. Mean stress at $N_f/2$.

EXPERIMENTAL DETAILS

Materials and Specimen

The specimen geometry used in this study was an hourglass configuration of the size shown in Figure 3. The materials examined in this program were Waspaloy, Wrought U 700 and PM U 700, as noted in Table 1. Hereafter they are designed as WA, WU, and PM, respectively. The WA and the WU were provided machined according to Figure 3, whereas blanks were provided for the PM material. Independently-determined chemistries and heat treatments provided by NASA-Lewis have been included in Table 2. Care has been taken to ensure the test section of the PM samples did not involve material used to can the powder.

The test section of each specimen was polished with successively finer grades of silicon carbide paper to produce a fine surface finish with finishing marks parallel to the longitudinal axis of the specimen. After completing all machining and polishing operations, the specimens were degreased with trichloroethylene, followed by reagent acetone. Immediately prior to installation in the test system, the specimen was recleaned with a reagent-grade acetone.

Apparatus and Procedure

All tests were conducted in one of two similar closed-loop servocontrolled electrohydraulic test systems. Samples were axially loaded. Diametral strain was controlled to produce the hysteresis loops shown schematically in Figure 1 through the use of the diametral strain-time histories shown in Figure 4.

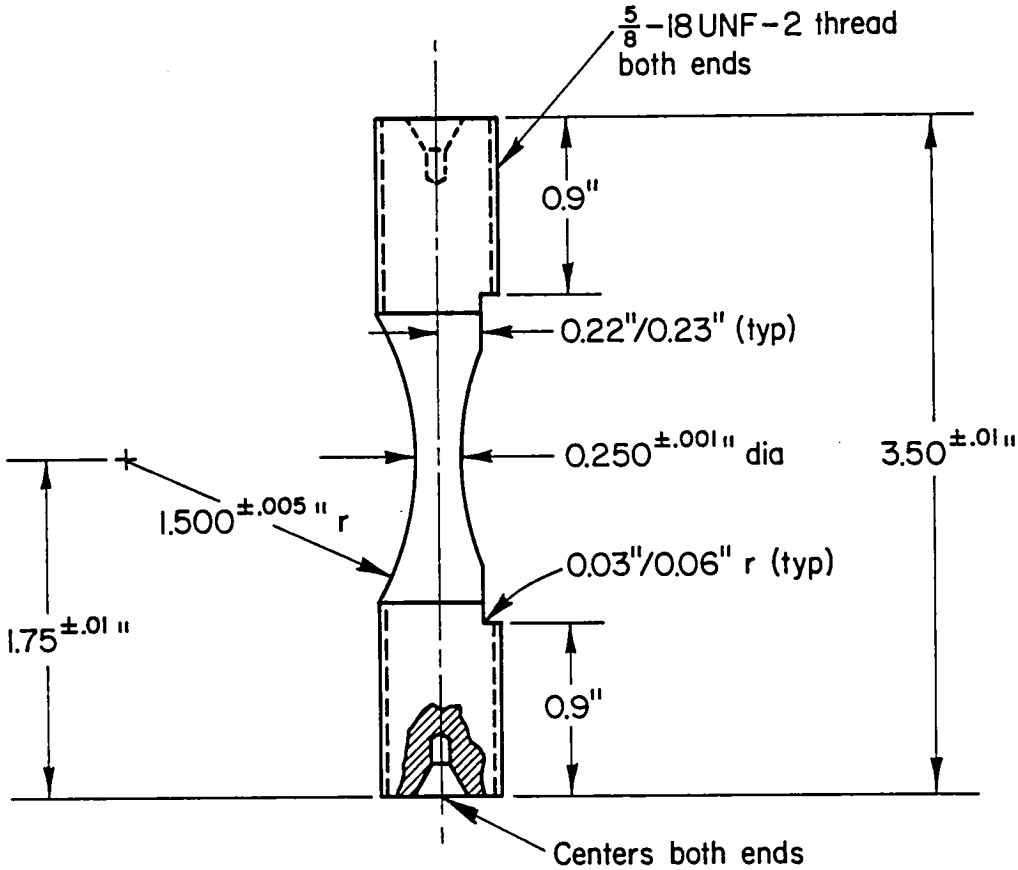

FIGURE 3. TEST SPECIMEN DESIGN

TABLE 2. COMPOSITIONS AND HEAT TREATMENTS OF THE MATERIALS STUDIED

	Waspaloy (WA)	Wrought U 700	PM U 700
	Nominal Composition in Weight % Unless Otherwise Noted		
C	0.039-0.042	.06-.07	0.06
Mn	< 0.10	< 0.10	< 0.1
Si	< 0.10	< 0.10	< 0.1
Cr	19.4-19.6	14.7-15.1	14.8-15.0
Ni	Balance	Balance	Balance
Co	VARIES: SEE TABLE 1 FOR DETAILS		
Fe	0.10-0.13	0.11-0.15	0.1-0.11
Mo	4.07-4.19	4.90-5.05	4.85-5.1
Ti	2.99-3.05	3.46-3.61	3.51-3.58
Al	1.29-1.33	4.05-4.14	4.0-4.08
B	0.004-0.005	0.022-0.028	0.019-0.026
Zr	0.07	0.04	0.06
S	0.003-0.004	0.002	0.002
P	< 0.01	< 0.01	< 0.01
Cu	< 0.10	< 0.01	< 0.10
O	-	4-11 ppm	41-64 ppm
N	-	10-16 ppm	11-18 ppm
Pb	-	-	<5 ppm
Bi	-	-	< 0.5 ppm
	Solution Treat Age and Anneal		
	S1015°C/4H-Q 840°C/4H-AC 760°C/16H-AC	S1130°C/4H-Q315°C; 870°C/8H-AC; 980°C/4H-AC; 650°C/24H-AC; 760°C/8H-AC	S1100°C/4H-Q; 870°C/8H-AC; 980°C/4H-AC; 650°C/24H-AC; 760°C/8H-AC.

S = solution treat, H = hours, Q = quench, AC = air cool

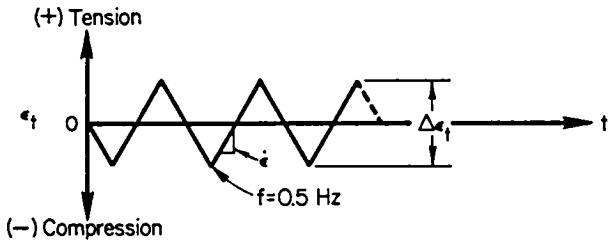

(a) Fully reversed strain-cycling wave form

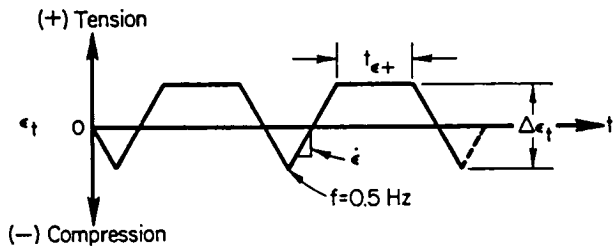

(b) Fully reversed strain-cycling wave form with maximum tensile strain hold time

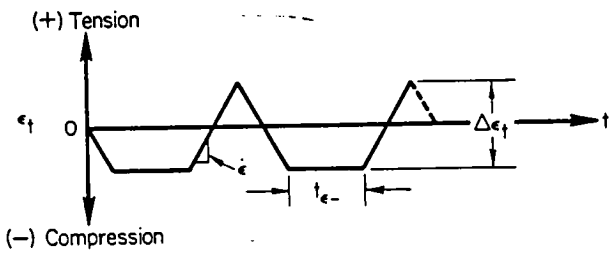

(c) Fully reversed strain-cycling wave form with maximum compressive strain hold time

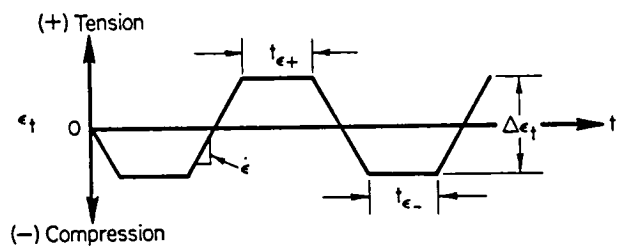

(d) Fully reversed strain-cycling wave form with tensile plus compressive strain hold time

FIGURE 4. DIAMETRAL STRAIN TIME HISTORIES

Diametral strain was controlled using the extensometer shown schematically in Figure 5. The diametral extensometer consisted of adjustable sensing arms of high purity alumina connected to a bracket consisting of two parallel beams joined by a flexible ligament that acts as an elastic hinge. For the arrangement used, diameter changes were mechanically multiplied by a factor of three before they are sensed at the other end of the extensometer by an LVDT. Load was measured with a commercial strain-gaged load cell mounted in series with the specimen.

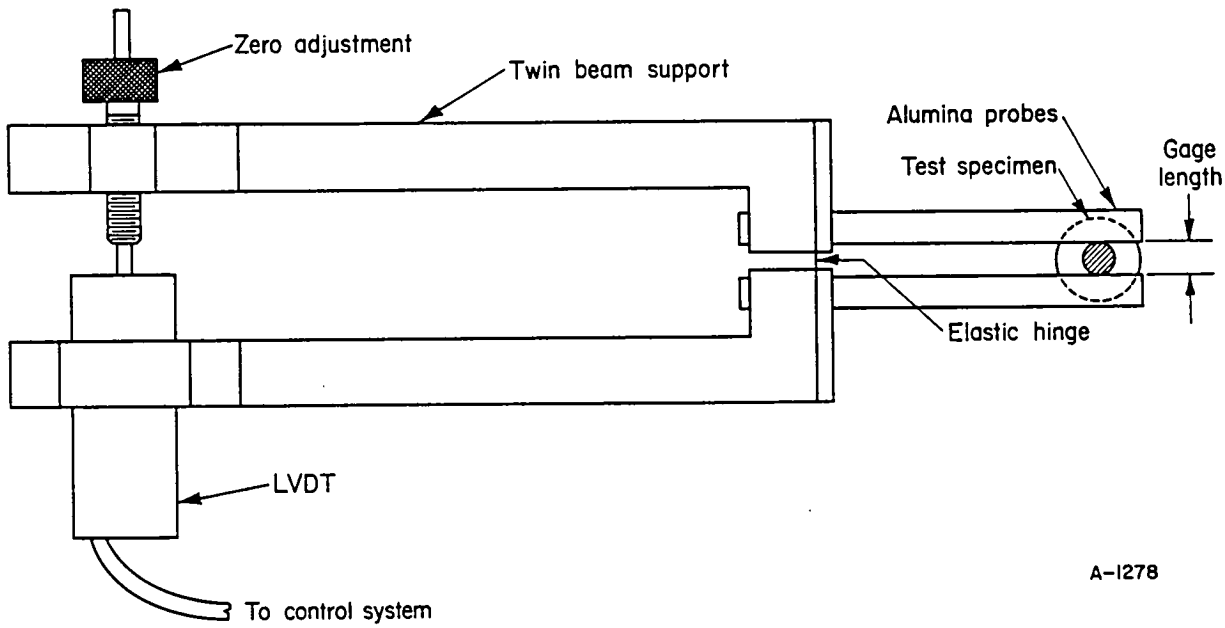

FIGURE 5. REPRESENTATION OF DIAMETRAL EXTENSOMETER

Calibration of the load cell was performed prior to and several times during the performance of the program. The load cell was protected from long term thermal drift and the development of thermal gradients through a circulating water system. The extensometer was calibrated to ASTM Class B for the small strain ranges of interest in this study. Independent studies verified the ability of the test system and extensometer (gain and hysteresis) to track waveforms comparable to those of Figure 4 within an error band of $\pm$ 1 percent. Difficulties with system stability at startup and at signal polarity changes were avoided by the use of isolation pads which interrupted the mechanical feedback.

Specimens were heated by high frequency induction and temperature was controlled by a commerical proportional-type power controller. Calibration of the test section temperature as a function of the shoulder temperature was performed for a variety of shoulder positions. The geometry of the coil was designed to minimize the thermal gradient in the vicinity of the midpoint of the hourglass specimen to reduce uncertainty in this calibration. Temperature feedback was provided by a thermocouple spotwelded to the shoulder of the specimen. Prior to each test, a loop-type thermocouple, looped about the test section, was used to fine tune this calibration on a specimen-to-specimen basis. Temperature was controlled to within ± 1 percent of the control value throughout the test.

Prior to testing samples for a given material in accordance with the test plan set forth in Figure 2, calculations were made to estimate the total strain range that would produce failure in about 10^4 cycles. Thereafter, the corresponding diametral total strain was estimated using the relationship

$$e_L^t = (1-2\nu)\,\frac{s}{E} - 2\,e_D^t \qquad (1)$$

In this equation e_L^t denotes total longitudinal strain, ν denotes the elastic Poisson's ratio (positive in this equation), s denotes stress, E denotes elastic modulus, and e_D^t denotes total diametral strain. Values for E and ν were obtained from the literature for the peak temperatures of interest[3].

The value of e_D^T to produce 10^4 cycles to failure was obtained through a trial-and-error process using continuous cycling data developed for medium to high cobalt content conditions. The initial value of e_D^t was guided by preliminary testing done at NASA-Lewis[2] and the literature[3-8]. Unfortunately, several iterations were involved for all materials because the value of e_D^t depends on E and ν as evident in Equation (1). Specimen-to-specimen variations in E and ν therefore will cause variability in e_D^t for a given e_L^t associated with 10^4 cycles to failure. This means that the present study of the effect of cobalt content on fatigue resistance must be based on comparisons of lives developed at equal values of diametral strain rather than axial strain. Consideration

must also be given to scatter in the ratio of plastic to elastic strains calculated via Equation (1).

Since plastic strain tends to be a key driver for the fatigue damage process, specimen-to-specimen scatter in the ratio of plastic to elastic strains will cause scatter in fatigue resistances when comparisons are based on total diametral strain. For this reason, it is desirable to run comparison tests under plastic rather than total strain control, provided that the magnitude of plastic strain is large enough to permit accurate control. For Waspaloy, plastic strains are on the order of the elastic strains and large enough to permit the specimen-by-specimen selection of the total strain needed to develop the value of plastic strain associated with 10^4 cycles to failure. However, for the wrought and powder metallurgy U 700, significant transients develop and the plastic strain is small compared to the total strain. The transient behavior coupled with the fact that the plastic strain is small compared to the total strains means that total strain cannot be chosen to achieve fixed plastic strain on a specimen-by-specimen basis. Test control therefore used total strain to achieve a constant initial plastic diametral strain for Waspaloy and total diametral strain for both U 700 materials.

The test plan of Figure 2 was carried out at the diametral strain range found to produce lives on the order of 10^4 cycles to failure. For the Waspaloy this value was a total strain to produce an initial plastic strain range nominally 0.00135. For wrought U 700 and PM U 700 total strain ranges nominally were 0.00345 and 0.00284, respectively. Test procedure involved tracking the standardized check list shown in abbreviated form in Table 3*. Following setup, care was taken to develop thermal stability prior to setting the extensometer, and again after setting the extensometer. The initial elastic cycling modulus check segment of the list was used in every test to provide a continuing independent check of the system calibration.

---

* The same check list is used in all cases, with minor variations introduced for plastic versus total strain control.

TABLE 3. CHECK LIST FOR COSAM TESTS

Date _____ Specimen Number _____

Operator _____ Load Frame _____

_____ 1. Engineer approval of validity of previous test on this frame.

_____ 2. Verify that ranges for load and strain signal conditioners match the programs needs.

_____ 3. Zero-suppress load cell with load train broken.

_____ 4. With the bypass open, verify value of the shunt cal for load.

_____ 5. Mount test specimen in load frame.

_____ 6. Adjust temperature control setting to give desired test temperature in center of specimen as measured by the loop thermocouple.

_____ 7. Cut loop thermocouple and mount extensometer on test specimen.

_____ 8. Monitor extensometer ouput and load cell output on strip chart recorder. When these outputs stabilize, the test is ready to start.

_____ 9. Check waveform and frequency (0.5 Hz) settings on function generator and adjust if necessary.

_____10. Set span and set-point to zero voltage.

_____11. Check again and where applicable the stability settings and adjust if necessary.

_____12. Check settings on error detectors and adjust if needed.

_____13. Put system in load control and close by-pass valve.

_____14. Mechanically zero the extensometer. Verify the value of the shunt cal for strain.

_____15. Zero suppress the extensometer with zero load and system in load control.

_____16. Prepare plotters to record load and strain.

_____17. Change control condition to strain control, taking appropriate precautions.

_____18. Set span and set-point to give one small amplitude cycle. Run and record one cycle.

TABLE 3. (Continued)

_____19. Check value of modulus from the plot. Contact the engineer in case of inappropriate results.

_____20. Set the span and the set-point to achieve the control parameter for the test.

_____21. Run and record one cycle, lift and move the pen on the recorder and mark new zero on chart at new position. The first cycle must be clear and unambiguous and match the control settings.

_____22. If an overstrain occurs, incrementally decrement the strain to zero, decrementing each half cycle.

_____23. Restart the test for continuous run. Adjust span to achieve the desired strain range. Zero suppress as necessary.

_____24. Record loops as directed by engineer.

RESULTS

Waspaloy at 538 C

Deformation and fatigue resistance data developed for the Waspaloy are presented in Table 4, for testing under diametral total strain range control to achieve a constant value of the plastic strain range in the first cycle. These data are plotted in Figure 6.

Figure 6(a) shows continuous cycle results on total strain-life to failure coordinates for a range of cobalt contents. This figure includes results developed in the present program as well as data for 500 < T < 760 C from the literature[5,6,8]. With reference to the higher temperature data (642 < T < 760 C) shown in this figure, the life range studied lies in the short-life to long-life transition region*. Data developed in this regime tend to show a strong increase in life with a small decrease in strain, leading to a broad spread in results. This, coupled with the lack of a systematic pattern in the fatigue resistance as a function of Co content, suggests the resistance for continuous cycling is not a strong function of the Co alloying.

Figure 6(b) presents the data shown in Figure 6(a) on plastic-strain versus life-to-failure coordinates (the long life results are omitted since plastic strain was not measured). Note that the data for this study lie along a single trend line. In light of this figure, Co content does not appear to influence the continuous cycling fatigue resistance, at least at 538 C. Finally, Figure 6(c) shows that this same conclusion is reached when failure is defined by first indication of cracking**.

Results developed for the hold time cycling are presented in Figure 6(d) and compared to the scatter band for the continuous

---

* Note the decreased life at 642 < T < 760 C as compared to 500 < T < 538 C evident in Figure 6(a). Certainly, this may be due to differences in the test temperature. But in cases where longitudinal and diametral lives are compared (9), the diametral data consistently live longer than the corresponding longitudinal data. Care therefore, should be exercised in interpreting these results.

** First indication of cracking is defined as the cycle for which an asymmetric load drop occurs.

TABLE 4. LCF RESULTS FOR WASPALOY AT 538 C

Specimen Number	N_o, cycles	N_i, cycles	N_5, cycles	N_{50}, cycles	N_f, cycles	$(\Delta\varepsilon_D^T)$	$(\Delta\varepsilon_D^e)_{N_f/2}$	$(\Delta\varepsilon_D^{In})_{N_f/2}$	$(\varepsilon_D^{creep})_{N_f/2}$	$(\Delta\sigma)_{N_f/2}$ MPa	$(\sigma^{relax})_{N_f/2}$ MPa	$(\sigma_{mean})_{N_f/2}$ MPa	Comments
							a. for 0.0% Cobalt						
D5-1947-1D-1	13,150	13,150	13,200	13,209	13,209	0.0022	0.0022	0.0	0.0	1356.94	0.0	0.0	Failed at the thermocouple weld. Continuous cycling test.
D5-1947-1D-2	3,765	3,765	4,250	4,521	4,594	0.00407	0.00277	0.0013	0.0	1621.7	0.0	-24.82	Tension hold test.
D5-1947-1D-3	7,350	7,401	7,500	7,854	7,854	0.00396	0.00271	0.00125	0.0	1603.09	0.0	-25.86	Continuous cycling test.
D5-1974-1D-4	2,915	2,937	2,964	2,967	2,967	0.00415	0.0028	0.00135	0.0	1613.43	0.0	-6.9	Compression hold test.
D5-1947-1D-5	2,246	2,458	2,356	2,458	2,458	0.00417	0.0024	0.00177	0.0	1496.42	0.0	-23.44	Symmetric hold test.
							b. for 45% Cobalt						
D5-1948-1B-1	29,560	29,580	29,585	29,595	29,595	0.0027	0.00226	0.00044	0.0	1516.9	0.0	-68.95	Continuous cycling test.
D5-1948-1B-2	7,589	7,676	7,705	7,711	7,711	0.00383	0.00259	0.00124	0.0	1599.64	0.0	0.0	Continuous cycling test.
D5-1948-1B-3	4,910	5,280	5,130	5,745	5,893	0.00383	0.00257	0.00126	0.0	1593.23	0.0	-55.16	Test interrupted three times due to problems with Wood's metal grip. Tension hold test.
D5-1948-1B-4	4,484	4,535	4,528	4,562	4,565	0.00381	0.00254	0.00127	0.0	1527.45	0.0	-22.06	Compression hold test. 103 continuous cycles were imposed in the test because of a bad function generator.
D5-1948-1B-5	3,087	3,538	3,585	3,585	3,585	0.00368	0.00243	0.00125	0.0	1518.42	0.0	-68.95	Symmetric hold test.
							c. for 9% Cobalt						
D5-1949-1A-1	1,618	1,828	1,909	1,920	1,933	0.00517	0.00279	0.00238	0.0	1682.38	0.0	-13.79	Continuous cycling test.
D5-1949-1A-2	3,063	3,227	3,266	3,274	3,274	0.004	0.00261	0.00139	0.0	1668.59	0.0	0.0	Continuous cycling test.
D5-1949-1A-3	8,697	8,958	8,974	9,092	9,095	0.00415	0.00268	0.00147	0.0	1613.43	0.0	-34.48	Tension hold test.
D5-1949-1A-4	2,523	2,633	2,668	2,774	2,774	0.0043	0.0027	0.0016	0.0	1629.98	0.0	-12.41	Compression hold test. Cyclic softening caused $\Delta\varepsilon_D^p$ to increase.
D5-1949-1A-5	2,384	2,417	2,384	2,417	2,417	0.00432	0.0025	0.00182	0.0	1595.78	0.0	-27.58	Symmetric hold test.
							d. for 13.5% Cobalt						
D5-1950-1B-1	6,950	7,070	7,115	7,145	7,145	0.00374	0.00247	0.00127	0.0	1668.59	0.0	-27.58	Continuous cycling test.
D5-1950-1B-2	2,605	2,618	2,693	2,766	2,775	0.00412	0.00271	0.00141	0.0	1634.12	0.0	-17.24	Continuous cycling test.
D5-1950-1B-3	4,480	4,650	4,590	4,725	4,725	0.00414	0.00271	0.00143	0.0	1664.38	0.0	-51.02	Tension hold test.
D5-1950-1B-4	1,670	1,670	1,710	1,724	1,724	0.0044	0.0027	0.0017	0.0	1653.56	0.0	-27.58	Compression hold Test. Cyclic softening increased $\Delta\varepsilon_D^p$.
D5-1950-1B-5	2,833	3,097	3,031	3,154	3,154	0.00413	0.00259	0.00154	0.0	1622.67	0.0	-8.27	Symmetric hold test.

$\Delta\varepsilon_D^T$: Total diametral strain range

N_o : Number of cycles to first indication of failure by cracking

N_i : Number of cycles to 10% drip in stabilized ratio of peak tensile stress to peak compressive stress

N_5 : Number of cycles to 5% drop in stabilized load range

N_{50} : Number of cycles to 50% drop in stabilized load range

$(\sigma^{relax})_{N_f/2}$: Stress relaxation per cycle at $N_f/2$

$(\sigma_{mean})_{N_f/2}$: Mean stress of $N_f/2$

$(\Delta\varepsilon_D^{In})_{N_f/2}$: Inelastic strain range at $N_f/2$

$(\Delta\sigma)_{N_f/2}$: Stress Range at $N_f/2$

$(\varepsilon_D^{creep})_{N_f/2}$: Creep strain per cycle at $N_f/2$

N_f : Number of cycles to failure by complete separation

$(\Delta\varepsilon_D^T)_{n_f/2}$: Total strain range of $N_f/2$

$(\Delta\varepsilon_D^e)_{N_f/2}$: Elastic strain range at $N_f/2$

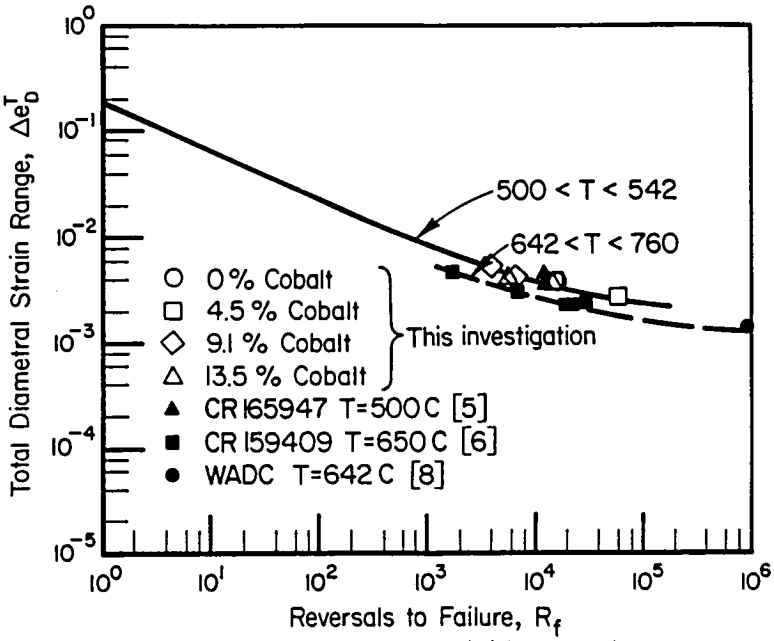

(a) Total diametral strain versus reversals to failure (separation) for continuous cycling

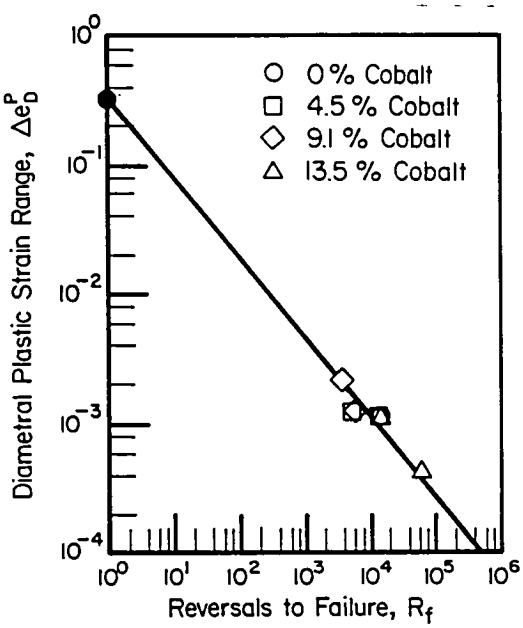

(b) Plastic diametral strain versus reversals to failure (separation) for continuous cycling

FIGURE 6. RESULTS DEVELOPED FOR WASPALOY AT 538 C AND 0.5 HZ

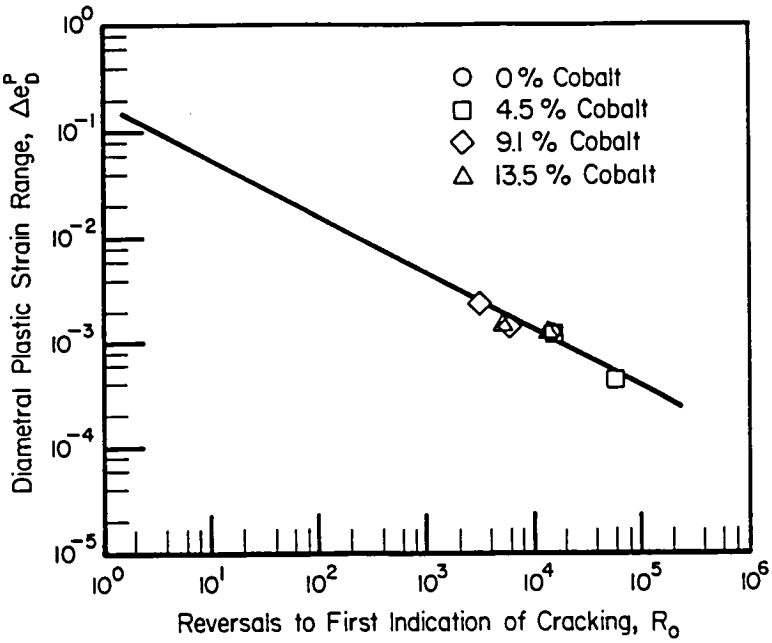

(c) Plastic diametral strain versus reversals to first indication of cracking for continuous cycling

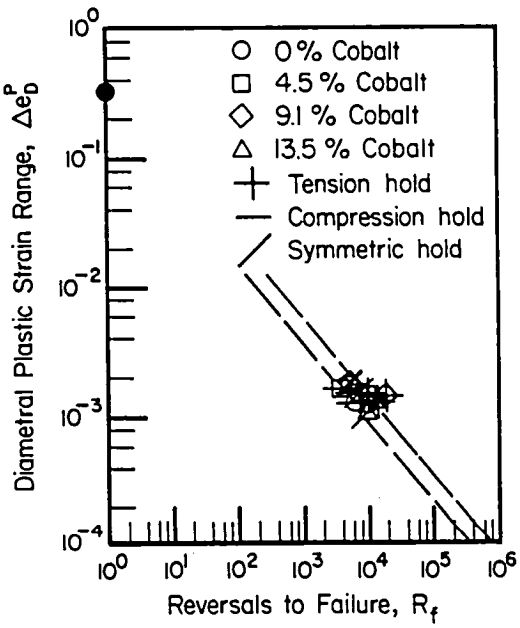

(d) Plastic diametral strain versus reversals to failure (separation) for hold time histories

FIGURE 6. (Continued)

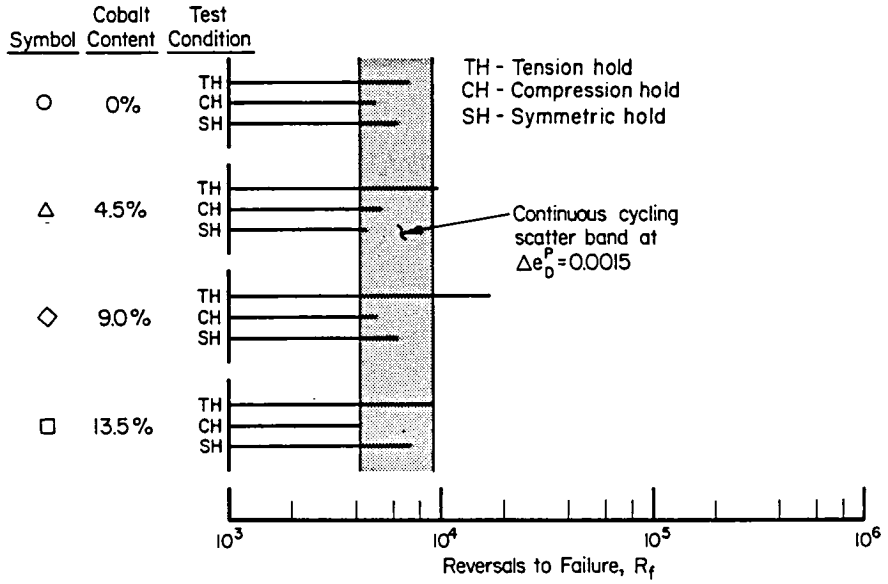

(e) Comparison of fatigue resistances as a function of cobalt content and strain history at $\Delta e_D^P = 0.0015$

FIGURE 6. (Concluded)

cycling data shown in Figure 6(b). These data show that (1) the bulk of these hold time data lie within the continuous cycling scatter band, (2) the tensile hold is less severe than the other holds, and (3) cobalt content has virtually no influence on the fatigue resistance of this material. These trends are more clearly evident on the bar graph of Figure 6(e) which represents fatigue resistance taken with reference to $e_D^P = 0.0015$.

Figure 7(a) shows a macroview of a failed specimen, taken from the 0% Co series and used to develop tension hold data. For this and most other Waspaloy specimens there is a small region associated with initiation and early cracking which is perpendicular to the maximum principle stress that subsequently transitions into a stable shear mode*. This Mode I initiation with a transition to Mode II growth is typical (in excess of 90%) of most specimens examined. Often the Mode II region occupies 90% of the area that develops stable cracking. Crack initiation and propagation appears to be transgranular in all cases examined, as shown for example for the 9% Co under continuous cycling in Figures 7(b)-(d). Note the macroscopic features reminiscent of striations in Figure 7(b)-(d). These features, which initially appear to mark macroscopic steps in the transition from Mode I to Mode II cracking, do not contain resolvable microscopic steps that could be associated with stepwise crack advance. In many cases the number of these features tends to correspond with the steps in reduction in load once a significant rate of load drop is established. Whether or not they are striations remains an open question.

Consider now the influence of hold times on the deformation response. Examination of the hysteresis behavior for all continuous cycling specimens tested indicates a slight initial softening followed

---

* Stable shear mode cracking can be ascribed to many mechanical factors. For example, insufficient lateral stiffness can produce the cracking behavior shown in Figure 7(a), either through bending in the load train or portal action in the load frame. Such action is not believed to be a factor in the present studies since this behavior was not experienced in past studies at comparable loads. More significantly, double (mirror symmetry across the plane of maximum principle stress) shear was observed in many cases. This action which cannot be explained through mechanical considerations suggests some material-related factor is responsible for the preference for Mode II cracking.

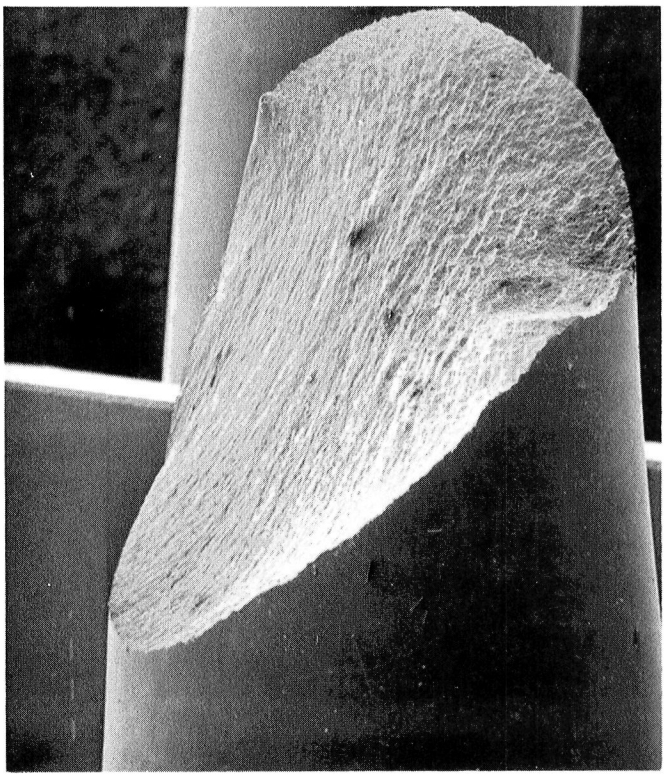

42598 SEM 10x

(a) Macroview of specimen D5-1947-1D-2; 0% Co alloy under tension hold cycling

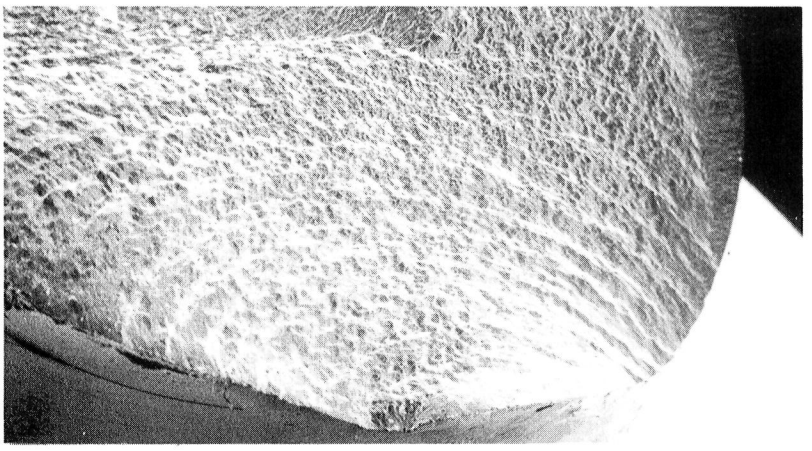

35692 SEM 5x

(b) Overview of fracture at origin in specimen D5-1949-1A-1; 9% Co alloy under continuous cycling

FIGURE 7. FRACTOGRAPHIC FEATURES FOR WASPALOY AT 538 C

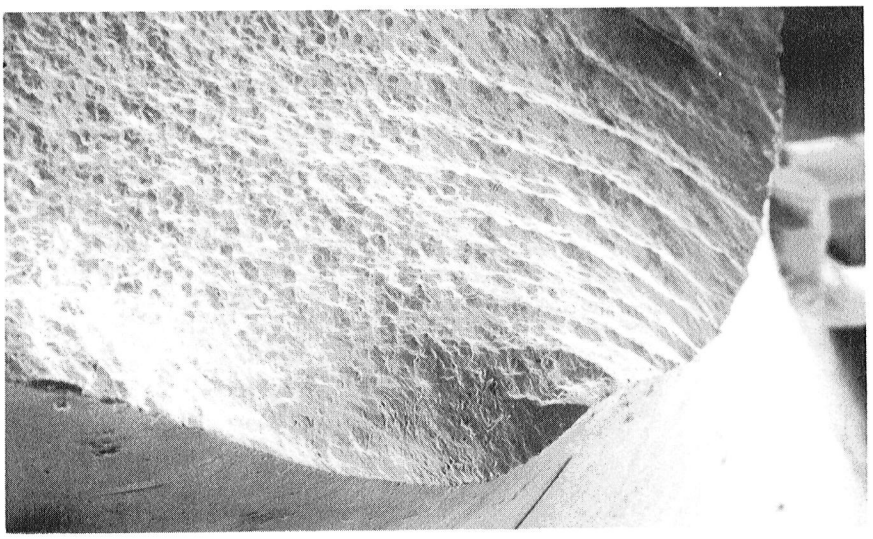

35691 SEM 25x

(c) Overview of fracture at origin in specimen D5-1949-1A-1; 9% Co alloy under continuous cycling

35693 SEM 100x

(d) Overview of fracture at origin in specimen D5-1949-1A-1; 9% Co alloy under continuous cycling

FIGURE 7. (Concluded)

by a slight hardening. An example of this behavior is shown in Figure 8(a). The imposition of hold times did not change this pattern. Hold times also did not influence the magnitude of the cyclic transient nor give rise to time dependent stress relaxation. However, in all hold time tests, each tip of the loop closed in a small tail, as evident on tensile loop tips for example in Figure 8(b). Detailed study of these loops indicate the trends observed could be explained in terms of the magnetomechanical effect[10]. The significance of the magneto-mechanical effect is explored later in Appendix A. We conclude there that it is not of great consequence.

The fact that hold times at peak tension/compression points in the deformation history did not cause time dependent flow is consistent with the apparently transgranular propagation and the similar lives developed for continuous cycling and hold time histories. This absence of time dependent flow precludes significant study of the influence of cobalt content if that cobalt is added to enhance creep resistance. On the other hand, we cannot conclude that cobalt is not significant to the creep-fatigue resistance of Waspaloy based on these tests at 538 C.

Powder Metallurgy U 700 at 760 C

Deformation and fatigue resistance data for the PM U 700 are presented in Table 5, for tests conducted under diametral total strain range control. These data are plotted in Figure 9.

Figure 9(a) presents continuous cycle results as open symbols on total-strain versus life-to-failure coordinates for the range of cobalt contents studied. As with the results for Waspaloy, all data presented appear to lie at or near the transition between finite and infinite life. Slight scatter in control condition or material in this transition region will strongly influence the fatigue resistance, making clear-cut interpretation of limited data difficult. This difficulty aside, data developed in this study, at cobalt contents of 12.7% and under, cluster at lives in excess of the trend for 17% Co. (In contrast, very sparse data developed at NASA-Lewis show 17% Co Wrought U 700 has the greatest fatigue resistance.)

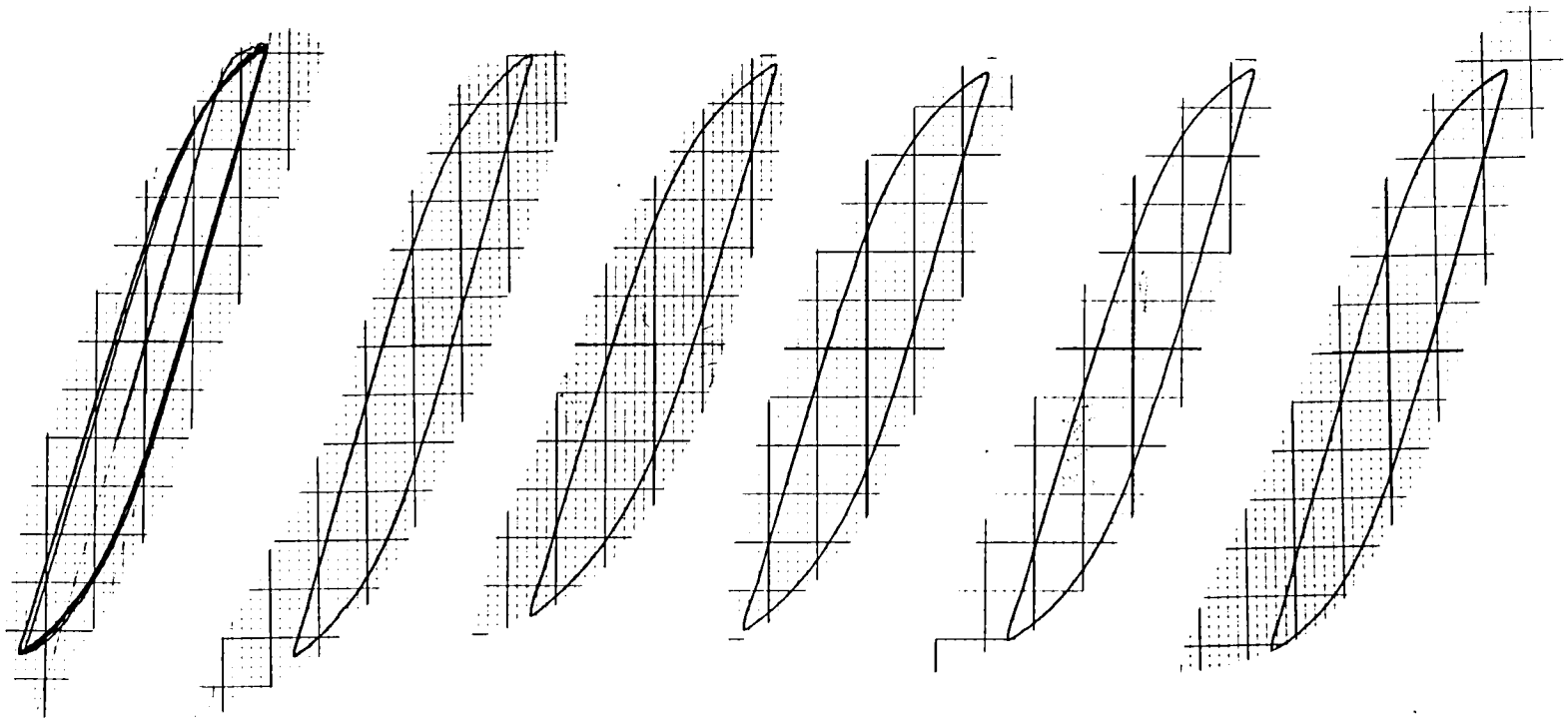

(a) Slight softening followed by hardening - continuous cycling - D5-1947-1D-3

FIGURE 8. TYPICAL CYCLIC DEFORMATION BEHAVIOR FOR WASPALOY AT 538 C

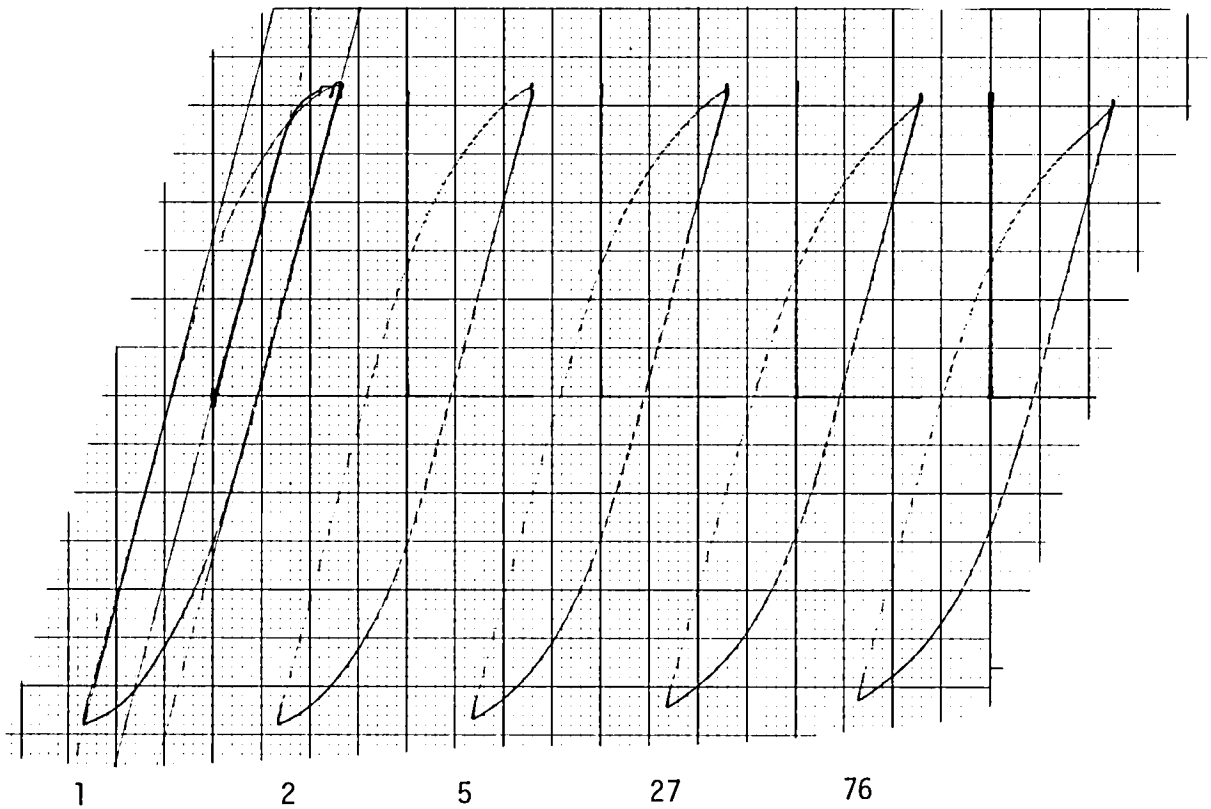

(b) Example of loop tip hysteresis - tension hold - D5-1950-1B3

FIGURE 8. (Concluded)

TABLE 5. LCF RESULTS FOR POWDER MET U 700 AT 760 C

Specimen Number	N_0, cycles	N_i, cycles	N_5, cycles	N_{50}, cycles	N_f, cycles	$(\Delta\varepsilon_D^T)$	$(\Delta\varepsilon_D^e)_{N_f/2}$	$(\Delta\varepsilon_D^{in})_{N_f/2}$	$(\varepsilon_D^{creep})_{N_f/2}$	$(\Delta\sigma)_{N_f/2}$ MPa	$(\sigma^{relax})_{N_f/2}$ MPa	$(\sigma_{mean})_{N_f/2}$ MPa	Comments
							a. for 0% Cobalt						
801374-74-1-1	2,762	2,912	2,812	2,971	2,971	0.00287	0.0026	0.00027	0.0	1451.4	0.0	-12.07	Continuous cycling test.
801374-74-1-2	4,327	4,361	4,361	4,361	4,361	0.00286	0.00257	0.00029	0.0	1436.71	0.0	-34.2	Continuous cycling test.
801374-74-1-3	2,047	1,807	2,100	2,327	2,327	0.00283	0.00254	0.00057	0.00028	1343.01	156.59	-182.72	Tension hold test.
801374-74-1-4	717	717	717	717	717	0.00284	0.00257	0.00051	0.00024	1287.3	128.94	150.66	Compression hold test.
801374-74-1-5	840	850	850	850	850	0.00284	0.00267	0.00125	0.000537 (Tension) 0.000521 Compression	1507.25	328.89 (Tension) 306.83 Compression	-41.09	Tension + Compression hold test.
							b. for 4.3% Cobalt						
801376-76-1-1	3,283	3,283	3,283	3,283	3,283	0.00275	0.00255	0.0002	0.0	1403.89	0.0	-34.48	Continuous cycling test.
801376-76-2-2	4,560	4,606	4,622	4,622	4,622	0.00284	0.00255	0.00029	0.0	1370.52	0.0	0.0	Continuous cycling test.
801376-76-2-3	3,022	3,452	3,452	3,622	3,622	0.00284	0.00255	0.00047	0.00018	1310.05	112.39	-187.54	Tension hold test. Bad function generator put 250 continuous cycles during early part of the test. These cycles not counted here.
801376-76-2-4	1,166	1,215	1,254	1,254	1,254	0.00285	0.00257	0.000417	0.00014	1335.01	84.95	146.66	Compression hold test.
801376-76-3-5	1,069	1,239	1,179	1,314	1,314	0.00284	0.00256	0.00102	0.000395 (Tension) 0.000348 Compression	1425.61	222.09 (Tension) 227.54 Compression	-27.58	Tension + compression hold test.
							c. for 8.55% Cobalt						
801379-79-1-1	60,205	60,205	60,205	60,205	60,205	0.0022	0.00211	0.000087	0.0	1164.22	0.0	-68.26	Continuous cycling test. Specimen overloaded then incrementally stepped down to zero. Test then accelerated.
801379-79-1-2	5,937	6,112	5,937	6,134	6,134	0.00266	0.00238	0.00028	0.0	1318.32	0.0	-8.27	Continuous cycling test.
801379-79-2-4	1,436	1,496	1,486	1,712	1,712	0.0028	0.00256	0.00036	0.00012	1343.15	82.26	137.21	Compression hold test.
801379-79-1-3	1,243	1,368	1,298	1,394	1,407	0.00285	0.00258	0.0004	0.000134	1342.46	95.84	150.31	Compression hold.
801379-79-2-5	802	814	812	827	827	0.00284	0.00261	0.00102	0.00044 (Tension) 0.00035 Compression	1478.98	273.87 (Tension) 221.88 Compression	-13.79	Tension + compression symmetric hold.

TABLE 5. (Continued)

Specimen Number	N_o, cycles	N_i, cycles	N_5, cycles	N_{50}, cycles	N_f, cycles	$(\Delta\varepsilon_D^T)$	$(\Delta\varepsilon_D^E)_{N_f/2}$	$(\Delta\varepsilon_D^{in})_{N_f/2}$	$(\varepsilon_D^{creep})_{N_f/2}$	$(\Delta\sigma)_{N_f/2}$ MPa	$(\sigma^{relax})_{N_f/2}$ MPa	$(\sigma_{mean})_{N_f/2}$ MPa	Comments
							d. for 12.7% Cobalt						
801380-80-2-1	2,917	2,963	2,978	2,990	2,990	0.0031	0.00246	0.000625	0.0	1463.26	0.0	-31.03	Continuous cycling test.
801380-80-3-2	1,280	2,049	1,510	2,049	2,049	0.00318	0.00258	0.0006	0.0	1430.71	0.0	-12.06	Continuous cycling test.
801380-80-3-3	3,642	3,708	3,708	3,708	3,708	0.00285	0.00256	0.000443	0.000158	1351.01	109.84	-196.61	Tension hold test.
801380-80-3-4	1,101	1,465	1,346	1,530	1,546	0.00284	0.00260	0.000316	0.000079	1395.69	82.12	121.77	Compression hold test.
801380-80-3-5	980	990	883	1,098	1,098	0.00284	0.00268	0.0007	0.00024 (Tension) 0.0003 Compression	1477.6	186.17 (Tension) 155.83 Compression	-27.58	Tension + compression hold test.
							e. for 17% Cobalt						
801382-82-1-1	44	85	85	92	92	0.0081	0.0038	0.0043	0.0	2170.55	0.0	-42.75	Continuous cycling test.
801382-82-1-2	1,145	1,775	1,538	1,829	1,829	0.00305	0.00255	0.0005	0.0	1405.2	0.0	-17.24	Continuous cycling test. (Defect seems to be present near cracking site.)
801382-82-1-3	-	-	-	-	-	-	-	-	-	-	-	-	Invalid tension hold test. Specimen overloaded.
801382-82-1-4	842	878	879	913	930	0.00281	0.00262	0.000252	0.000063	1354.66	41.03	61.57	50 cycles of symmetric hold applied by error during the test. COMPRESSION HOLD. (Loops not very clean so may be error.)
801382-82-1-5	877	877	887	887	887	0.00284	0.00272	0.00066	0.00028 (Tension) 0.00026 Compression	1456.22	163.86 (Tension) 148.38 Compression	-27.58	Symmetric hold.

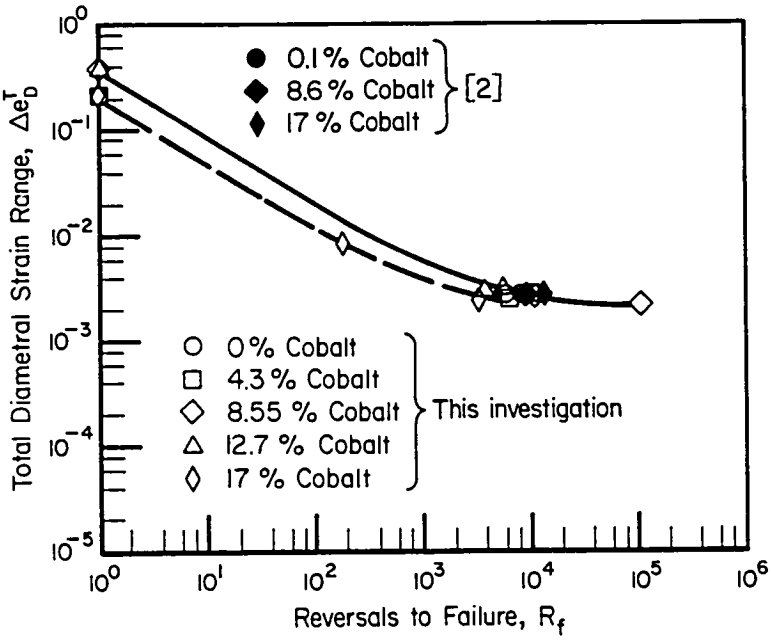

(a) Total diametral strain versus reversals to failure (separation) for continuous cycling

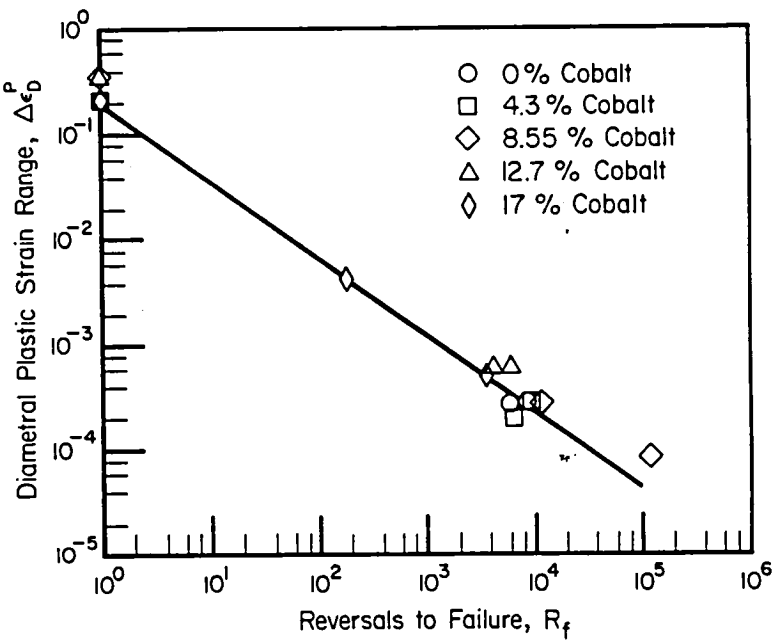

(b) Plastic diametral strain versus reversals to failure (separation) for continuous cycling

FIGURE 9. RESULTS DEVELOPED FOR PM U 700 AT 760 C AND 0.5 HZ

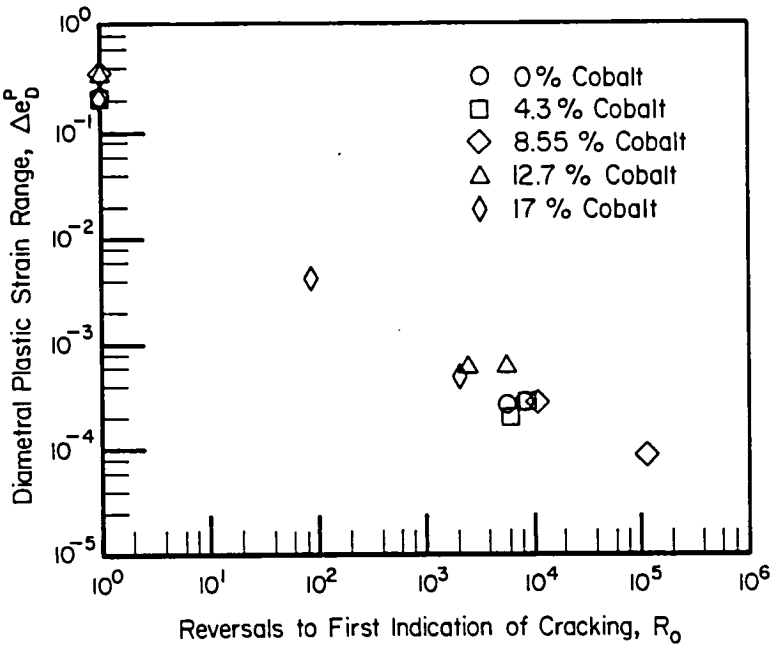

(c) Plastic diametral strain versus reversals to first indication of cracking for continuous cycling

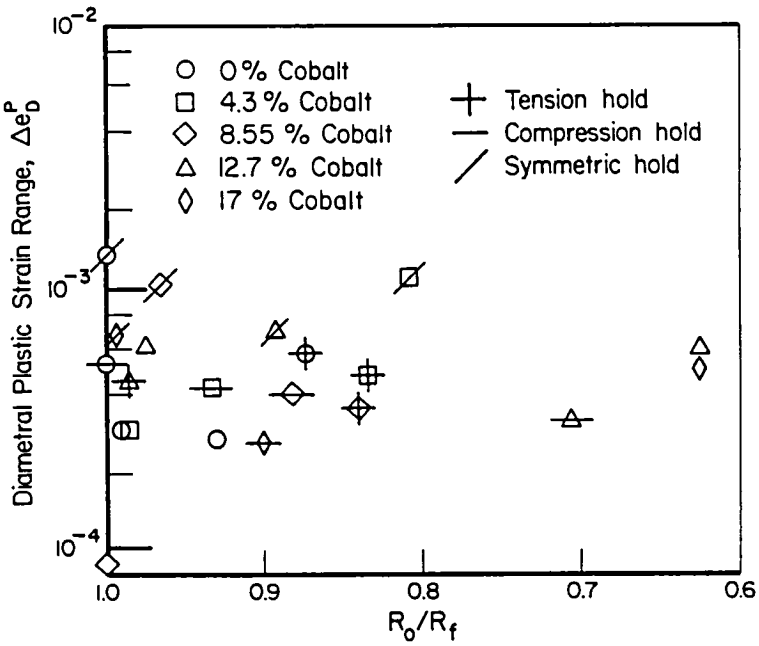

(d) Diametral plastic strain range versus the ratio of reversals to first detection to reversals to separation

FIGURE 9. (Continued)

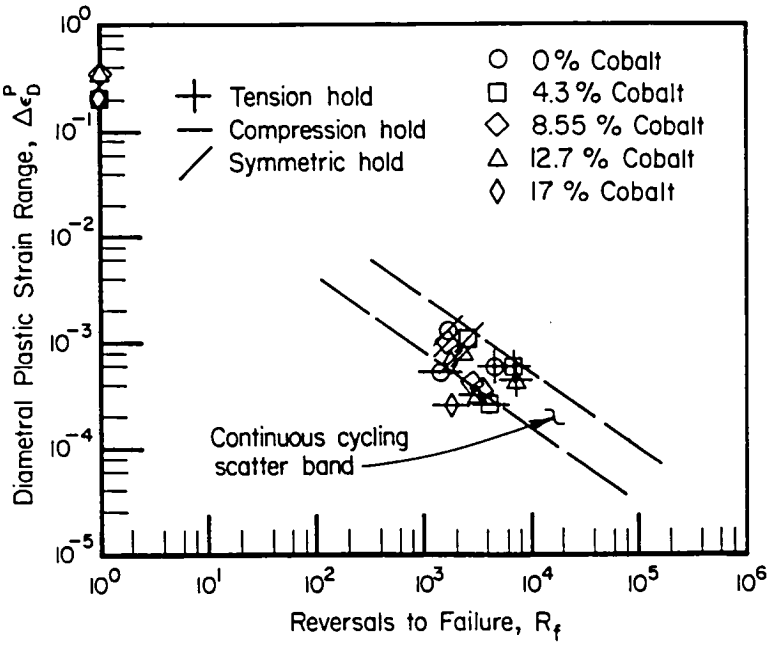

(e) Plastic diametral strain versus reversals to failure (separation) for hold time histories

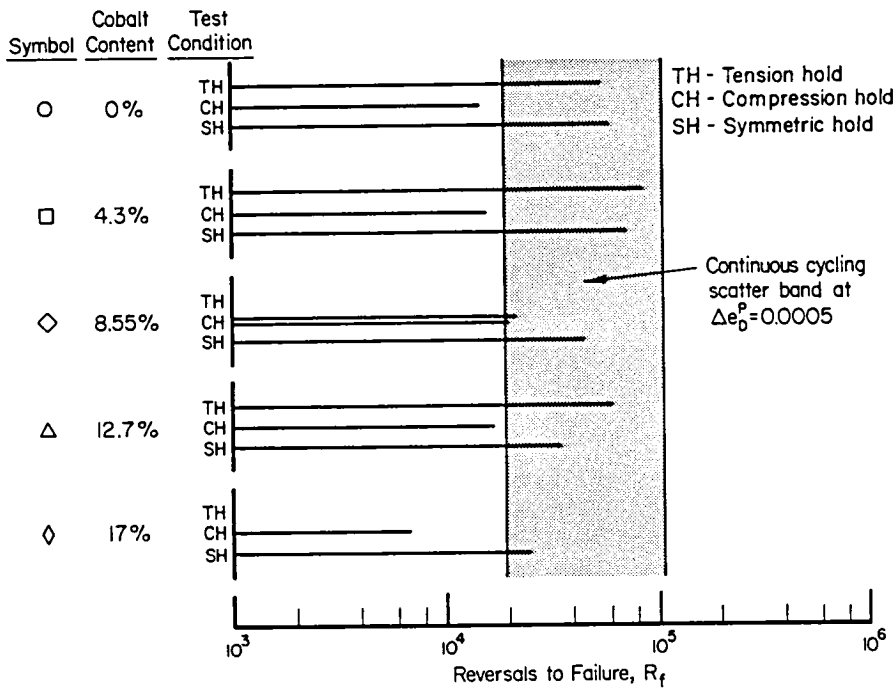

(f) Comparison of fatigue resistances as a function of cobalt content and strain history at $\Delta e_D^p = 0.0005$

FIGURE 9. (Concluded)

Trends in fatigue resistance with cobalt content are easier to discern when results are compared on coordinates of plastic-strain and life-to-failure, as evident in Figure 9(b). This figure indicates superior resistance is developed for 12.7 and 8.55 percent PM U 700. The fact that trends differ on plastic and total strain coordinates suggests that a choice must be made between these as to which controls the fatigue damage process. For the present, plastic strain will be used.

It has been established in the literature that the fraction of life spent in crack nucleation* is a function of the strain imposed. For the present program, total strain imposed was varied until the strain to produce 10^4 cycles to failure was empirically determined. Moreover, once total strain was determined, variation in material meant that plastic strain varied for fixed total strain. Since different mechanical parameters appear to control nucleation and growth, a bias may be introduced by the choice of failure criteria which admits a significant crack growth period. Possible bias due to the failure criterion can be explored by comparing the trends for results in terms of first indication of cracking, defined earlier and presented in Figure 9(c), with trends for separation just discussed and presented in Figure 9(b). Such a comparison indicates the choice of a failure criterion does not lead to different resistance trends. One might then conclude the definition of failure does not influence ranking by cobalt content of the resistance to nucleation or growth. Indeed as shown in Figure 9(d) data for the range of cobalt contents studied cluster at large values of the ratio of first indication of cracking, R_o, to total life, R_f. Unfortunately, the data are too sparse and cover too few values of R_o/R_f to support or deny conclusions regarding ranking crack growth resistance with cobalt content. But one can conclude that the trends drawn in light of Figure 9(b) are valid up to the formation of physically small cracks (~ 25 - 500 μm).

Results developed for hold-time cycling are presented in Figure 9(e) in comparison with the scatter band for continuous cycling data

---

* The absolute fraction spent in nucleation depends on the crack length chosen to define nucleation. but in all cases, once a criterion is selected, the literature shows that the fraction spent in nucleation depends on the strain range imposed.

(Figure 9(b)). As with the waspalloy, the bulk of the hold time data lie within the continuous cycling scatter band. Also, as with the waspalloy there is a banding in the results with the cycle type--tensile holds are less severe than symmetric holds, with the compression hold being most severe. Again as with the waspalloy, cobalt content has only a nominal influence on life, except at the highest cobalt content for which there appears a slight life reduction. These trends are clearly evident in Figure 9(f) which compares test results at a common plastic strain range of 0.0005. Note that the scatter in life for this PM material is somewhat greater than that for the waspalloy material.

Reasons which can account for a decrease of resistance with increased cobalt content include changes in microstructure (e.g. fracture morphology, crack initiation mechanism) and deformation response (e.g. ratio of elastic to plastic strain). Which of these is responsible is beyond the scope of the present study. Macroscopic (up to 35x) examination of fracture surfaces did not indicate major trends in initiation and growth behavior as a function of cobalt content or strain history. Typically, initiation occurred on a plane perpendicular to the maximum principal stress. Growth continued on that plane until separation resulting in the formation of a shear lip occurred. Fractography suggests that macrocrack growth occupied only a small fraction of the total life. Initiation most often occurred at a single site. In many cases initiation and growth occurred primarily between compacted particles, there being some evidence of planar-like transgranular growth. An example of initiation at a foreign particle is shown along with typical growth features in Figure 10.

Consider now the influence of cobalt content and hold times on the deformation response. Results show that the maximum stress tends to decrease slightly for continuous cycling, as shown in Figure 11(a). Similar trends are evident in Figures 11(b) and (c) for tension and symmetric holds respectively, with the greatest decreases occurring for the tension hold cycle. In contrast, Figure 11(d) indicates the maximum stress increases for fully reversed strain cycling with compression hold times. Given that the same total strain was involved in all tests, one might infer that the shortest lives would be associated with

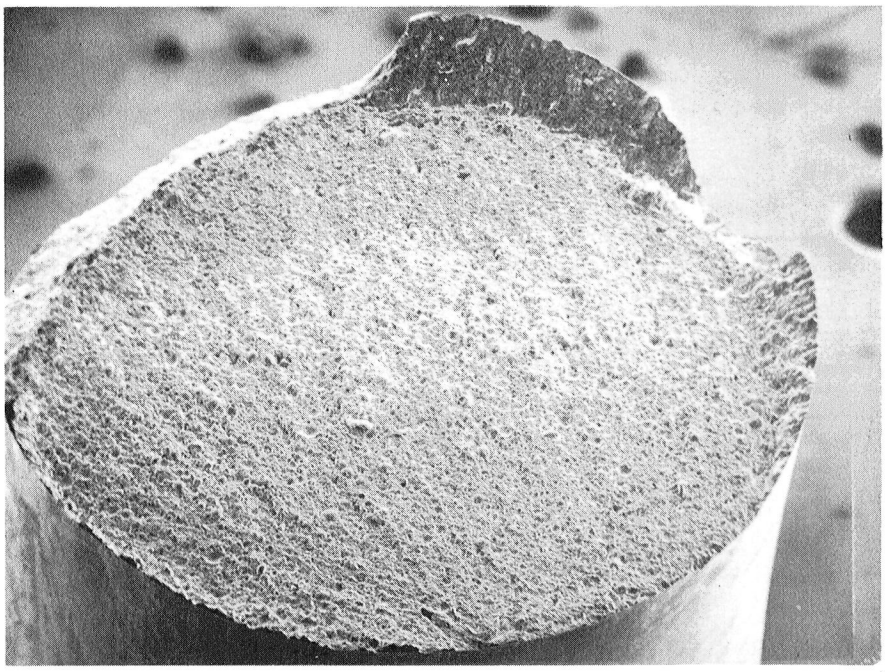

37800 SEM 14x

(a) Overview

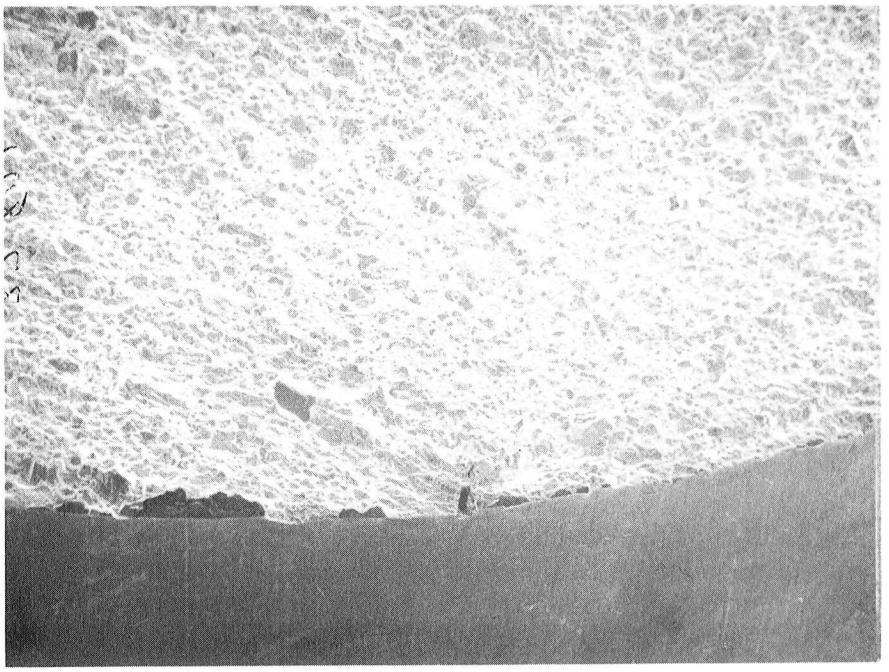

37801 SEM 50x

(b) View at initiation site

FIGURE 10. FRACTOGRAPHIC FEATURES OF PM U 700 SAMPLE 801382-82-1-2; CONTINUOUS CYCLING

37802 SEM 250x

(c) Detail at initiation site

FIGURE 10. (Concluded)

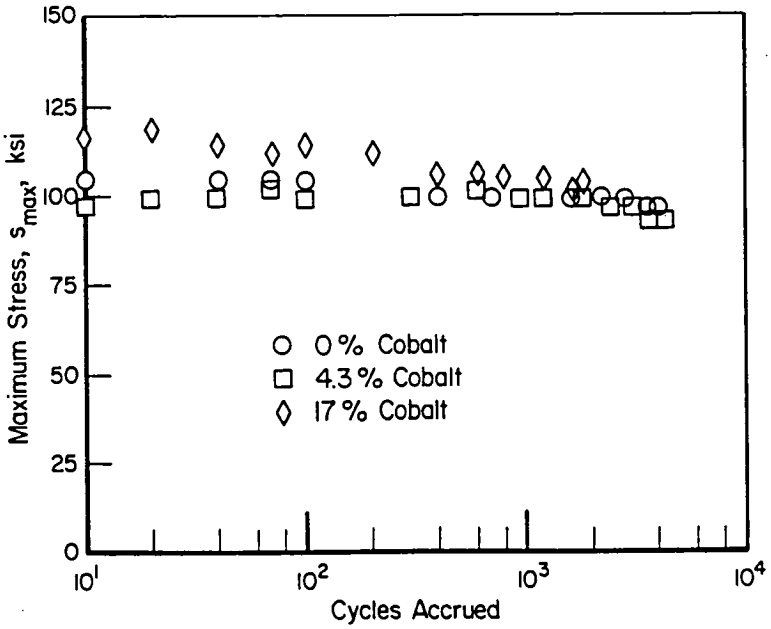

(a) Continuous cycling

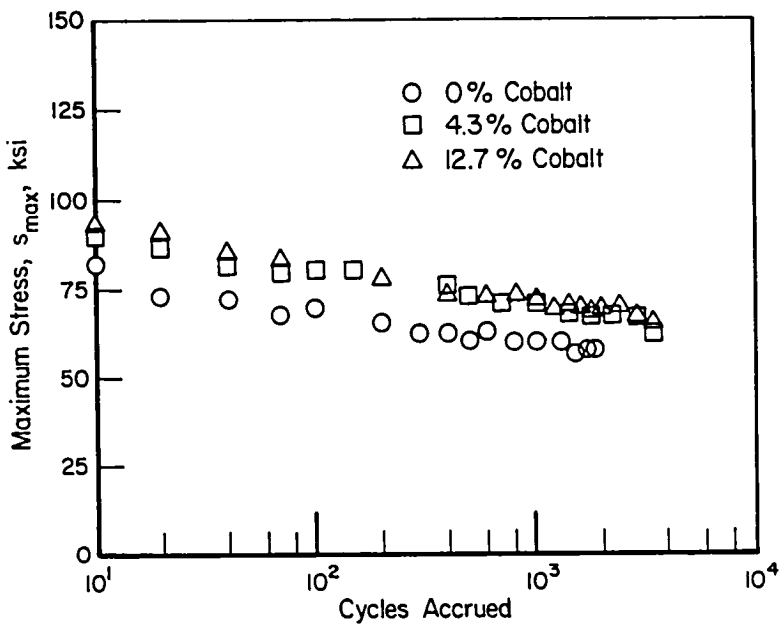

(b) Tension hold

FIGURE 11. TYPICAL DEFORMATION BEHAVIOR FOR EACH OF THE STRAIN HISTORIES FOR PM U 700 AT 760 C

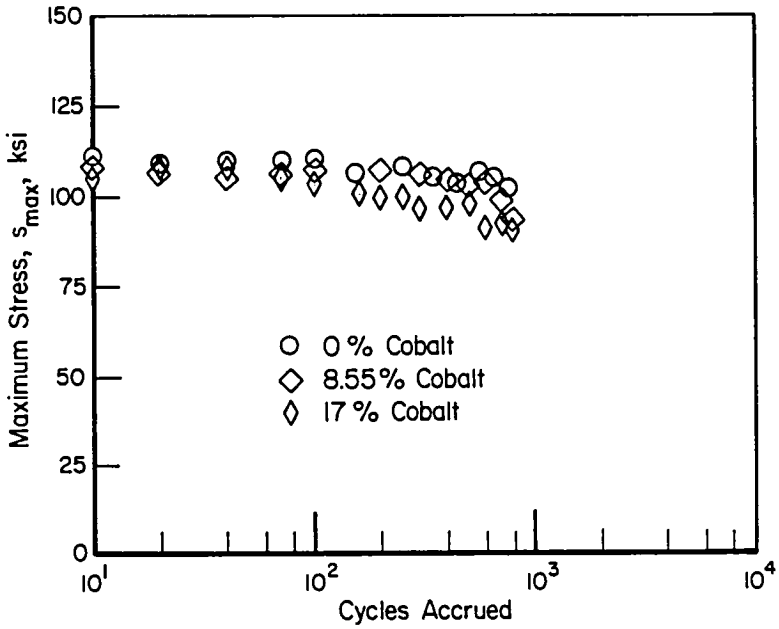

(c) Symmetric hold

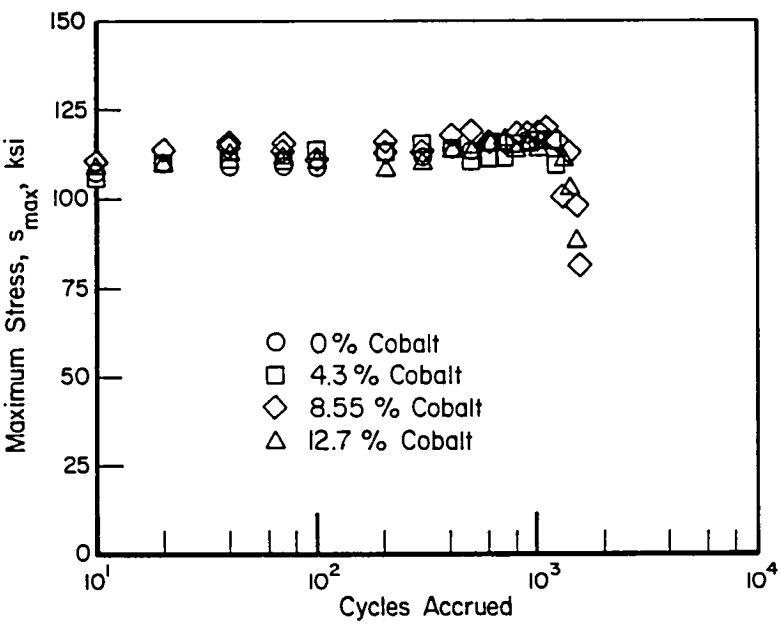

(d) Compression hold

FIGURE 11. (Continued)

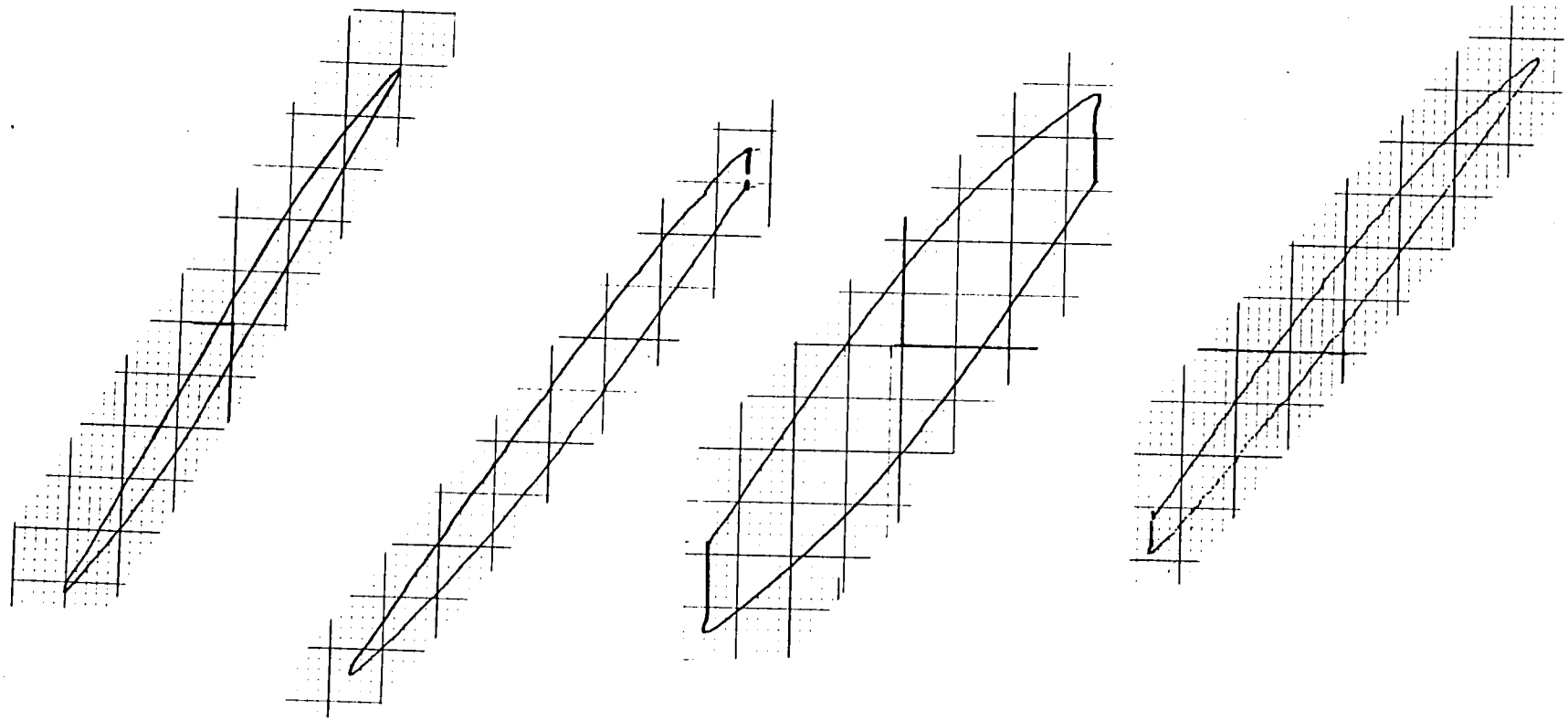

(e) Continuous cycling
8013-79-1-2;
1700 cycles

(f) Tension hold
8013-80-3-3;
1382 cycles

(g) Symmetric hold
8013-76-3-5;
669 cycles

(h) Compression hold
8013-79-2-4;
1444 cycles

FIGURE 11. (Concluded)

the highest maximum strains. In turn, this would suggest a criterion that includes maximum stress, such as $s_{mx}\ e_D^P$, would effectively consolidate these data. Unfortunately, life is not so simple. As maximum stress increases, e_D^P decreases due to hardening resulting in offsetting effects. The inclusion of s_{mx}, providing a complete deformation based fatigue criterion, thus does not embody the sequence dependence of the fatigue resistance of PM U 700.

The sequence dependence arises because the total damage leading to initiation involves contributions from time-independent as well as time-dependent mechanisms. The influence of the time dependence is evident in the stress relaxation or the creep strain recorded in Table 5. The stress relaxation behavior is contrasted for the strain histories involved in Figures 11(e) through (g). It is evident from the table that diametral creep strain per cycle, e_D^c, normalized with respect to the inelastic strain per cycle, e_D^P, tends to decrease with cobalt content for contents between 0 and 4.3 percent. Beyond 4.3 percent, the influence of cobalt is negligible, at least for 1 minute hold periods.

Wrought U 700 at 760 C

Deformation and fatigue resistance data for the Wrought U 700 are presented in Table 6. These results are presented in Figure 12. Observe from the table that for several specimens entries are included for N_0 and separation only. This situation arose because the magnitude of the asymmetric change in load drop was very small prior to specimen separation. The table also includes a number of entries for which separation occurred at lives well below the desired 10^4 cycles to failure even though the corresponding strain was based on available data[2]. This situation apparently arose because a number of samples contained major surface defects in the condition supplied. This is shown, for example, in Figure 13. For this reason, a number of specimens were returned to NASA for reworking at the discretion of our monitor, as set forth in Table 7. In view of the defects, the life of some specimens discussed may be largely cycles to grow a crack from a defect, whereas for other samples the life reported will also involve the number of cycles to initiate a dominant singularity. The implications of this difference are pursued later in this section.

TABLE 6. LCF RESULTS FOR WROUGHT U 700 AT 760 C

Specimen Number	N_0, cycles	N_i, cycles	N_5, cycles	N_{50}, cycles	N_f, cycles	$(\Delta\varepsilon_D^T)$	$(\Delta\varepsilon_D^e)_{N_f/2}$	$(\Delta\varepsilon_D^{in})_{N_f/2}$	$(\varepsilon_D^{creep})_{N_f/2}$	$(\Delta\sigma)_{N_f/2}$ MPa	$(\sigma^{relax})_{N_f/2}$ MPa	$(\sigma_{mean})_{N_f/2}$ MPa	Comments
							a. for 0.1% Cobalt						
D5-1884-4-1	850	-	-	-	1,635	0.004	0.0028	0.0012	0.0	1582.75	0.0	0.0	Continuous cycling test. Large amount of softening.
D5-1884-4-2	2,457	-	-	-	2,507	0.00345	0.00275	0.0007	0.0	1502.08	0.0	-19.31	Continuous cycling test. No change in load response with cycles.
D5-1884-5-3	845	900	900	932	932	0.0033	0.0026	0.0011	0.00038	1415.54	220.64	-166.51	Tension hold test.
D5-1884-9-4	279	-	-	-	296	0.00347	0.00273	0.00111	0.00037	1451.88	202.71	150.66	Compression hold test. No change in load response with cycles.
D5-1884-9-5	260	267	267	267	267	0.00346	0.00283	0.00197	0.00071 (Tension) 0.00063 Compression	1475.81	397.84 (Tension) 384.05 Compression	-30.34	Symmetric hold test.
							b. for 4.3% Cobalt						
D5-1885-3-1	5,000	-	-	45,000	45,063	0.00255	0.0023	0.000251	0.0	1244.06	0.0	0.0	Continuous cycling test. Large amount of softening.
D5-1885-6-2	1,440	-	-	2,514	2,514	0.00342	0.00285	0.00057	0.0	1588.33	0.0	0.0	Continuous cycling test.
D5-1885-6-3	1,200	1,824	1,814	-	1,929	0.0034	0.0027	0.0011	0.0004	1462.15	241.33	-221.33	Tension hold test.
D5-1885-11-4	75	-	-	-	233	0.00348	0.00279	0.001	0.00031	1531.93	193.61	151.69	Compression hold test. No change in stress response with cycles.
D5-1885-11-5	160	320	319	-	324	0.00338	0.00295	0.00164	0.00061 (Tension) 0.0006 Compression	1695.48	335.44 (Tension) 335.44 Compression	141.37	Symmetric hold test.
							c. for 8.6% Cobalt						
D5-1886-7-1	2,952	3,252	3,177	3,575	3,575	0.00327	0.00279	0.000483	0.0	1518.62	0.0	-7.93	Continuous cycling. Values are not quite half life values. Defect in specimen suspected to have produced low life value.
D5-1886-7-2	2,500	3,037	2,998	3,186	3,186	0.0034	0.00275	0.00065	0.0	1489.8	0.0	-13.79	Continuous cycling test.
D5-1886-7-3	1,200	-	-	-	2,304	0.00351	0.000286	0.00097	0.00032	1571.23	199.96	-209.61	Tension hold test. The machine shutdown and the test was restarted. Stress response never showed a decrease with cycles.
D5-1886-7-4	330	469	469	-	531	0.00343	0.00291	0.0007	0.00018	1607.22	120.66	133.76	Compression hold test.
D5-1886-9-5	160	543	513	-	579	0.00348	0.00306	0.00132	0.0005 (Tension) 0.0004 Compression	1714.15	307.24 (Tension) 231.67 Compression	-34.48	Symmetric hold test.

TABLE 6. (Continued)

Specimen Number	N_o, cycles	N_i, cycles	N_5, cycles	N_{50}, cycles	N_f, cycles	$(\Delta\varepsilon_D^T)$	$(\Delta\varepsilon_D^e)_{N_f/2}$	$(\Delta\varepsilon_D^{in})_{N_f/2}$	$(\varepsilon_D^{creep})_{N_f/2}$	$(\Delta\sigma)_{N_f/2}$ MPa	$(\sigma^{relax})_{N_f/2}$ MPa	$(\sigma_{mean})_{N_f/2}$ MPa	Comments
							d. for 12.8% Cobalt						
2-2-6-1	1,250	1,629	1,614	2,134	2,150	0.003	0.00276	0.00024	0.0	1509.32	0.0	-13.79	Continuous cycling test. Defect reduced life of specimen.
2-2-6-2	570	1,337	1,337	1,421	1,421	0.0034	0.000284	0.00056	0.0	1660.45	0.0	-17.24	Continuous cycling test.
2-2-9-3	175	1,755	1,695	-	2,057	0.00346	0.00287	0.00086	0.00027	1583.09	181.34	-189.61	Tension hold test.
2-2-9-4	317	377	367	-	457	0.00345	0.00288	0.00078	0.00021	1695.48	131.01	125.49	Compression hold test.
2-2-9-5	284	379	344	-	424	0.0035	0.0030	0.00124	0.00038 (Tension) 0.0004 Compression	1754.78	248.22 (Tension) 231.67 Compression	-38.61	Symmetric hold test.
							e. for 17% Cobalt						
3-1-10-1	4,500	-	-	-	23,110	0.0027	0.00255	0.000153	0.0	1413.96	0.0	-13.79	Continuous cycling test. Recorder ran out of chart paper overnight.
3-1-10-2	1,620	1,800	1,860	-	2,048	0.0035	0.00293	0.00057	0.0	1590.95	0.0	0.0	Continuous cycling test.
3-1-10-3	390	1,730	1,730	-	1,872	0.00345	0.00297	0.00076	0.00028	1628.6	151	-215.68	Tension hold test.
3-2-10-4	202	341	335	-	357	0.00354	0.00292	0.00086	0.00024	1635.15	137.42	144.11	Compression hold test.
3-2-10-5	284	411	331	-	435	0.00346	0.00271	0.00135	0.00033 (Tension) 0.00027 Compression	1806.83	271.32 (Tension) 244.15 Compression	-40.68	Bad specimen.

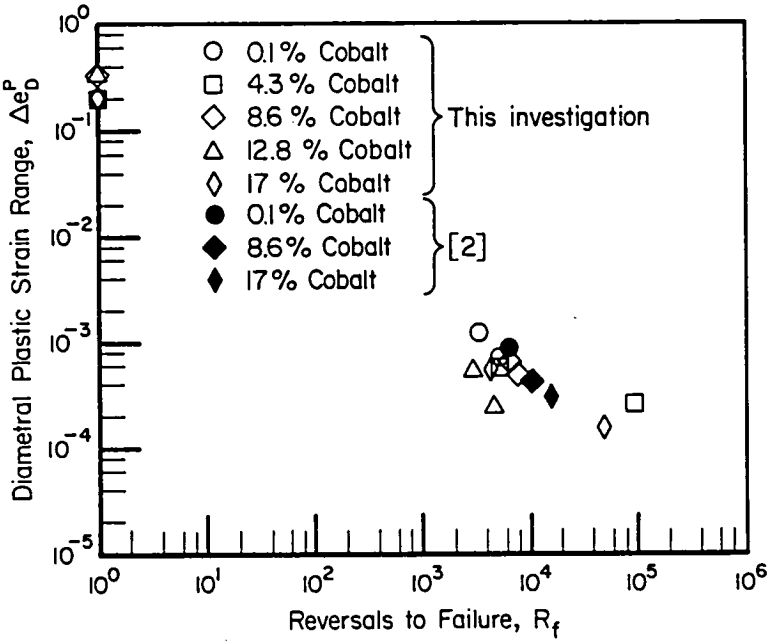

(a) Plastic diametral strain versus reversals to failure (separation) for continuous cycling

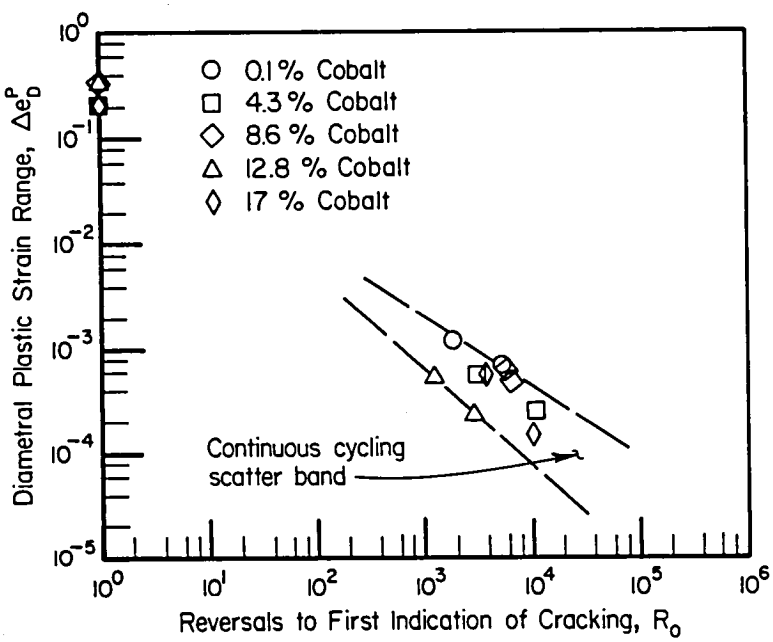

(b) Plastic diametral strain versus reversals to first indication of cracking for continuous cycling

FIGURE 12. RESULTS DEVELOPED FOR WROUGHT U 700 AT 760 C AND 0.5 HZ

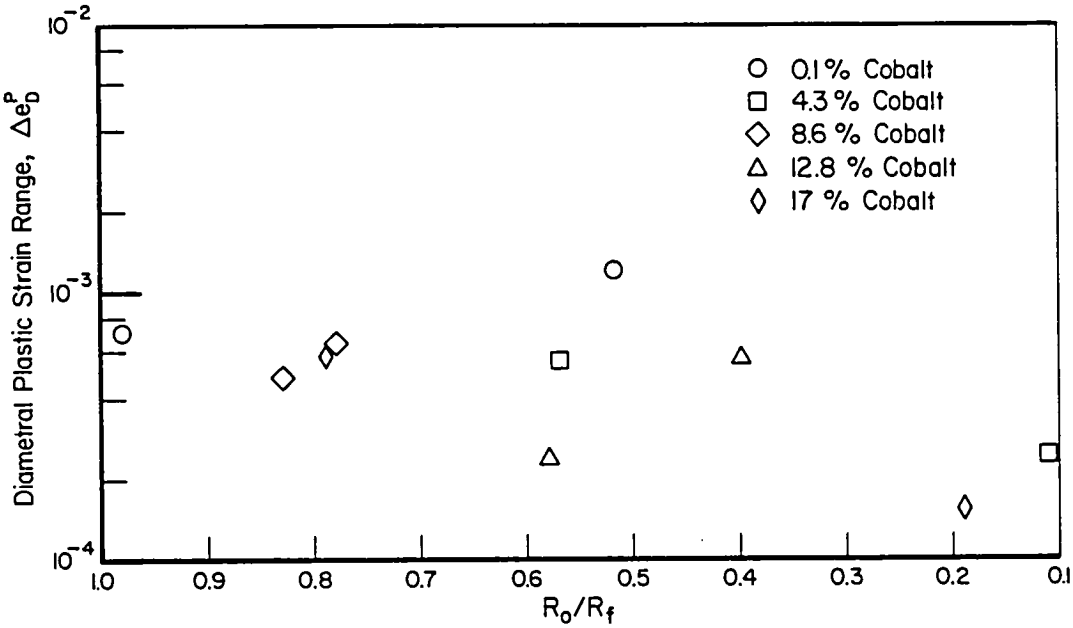

(c) Diametral plastic strain range versus the ratio of reversals to first detection to reversals to separation for continuous cycling

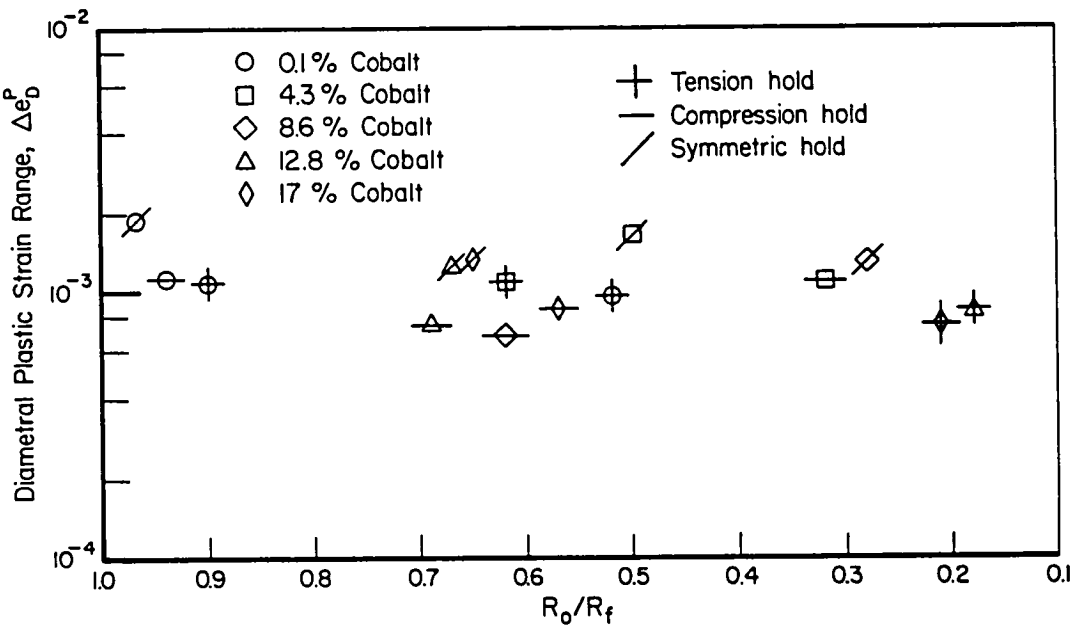

(d) Diametral plastic strain range versus the ratio of reversals to first detection to reversals to separation for hold time histories

FIGURE 12. (Continued)

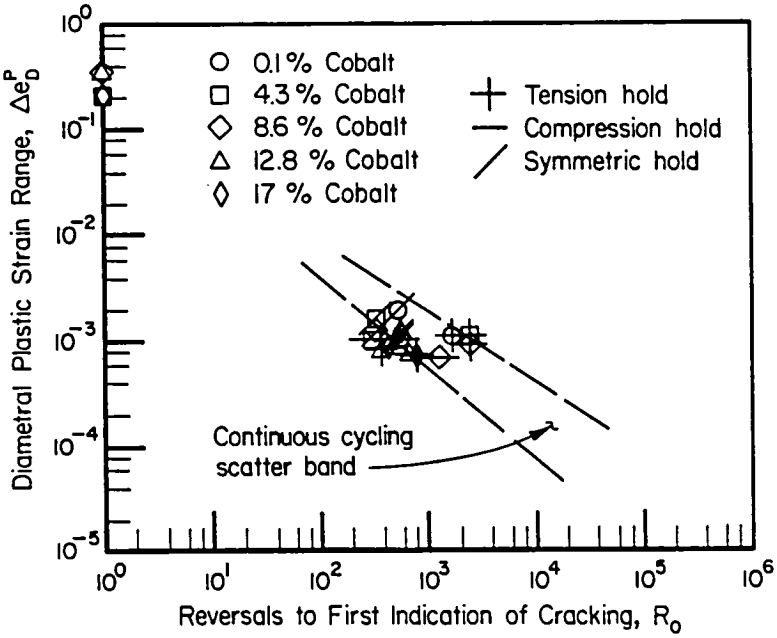

(e) Plastic diametral strain versus reversals to first indication of cracking for hold time histories

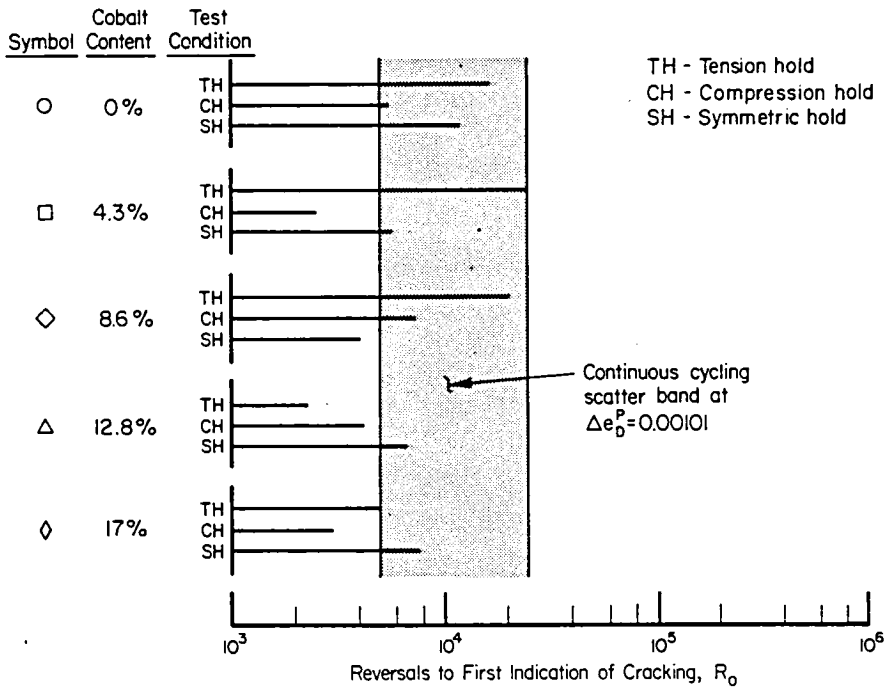

(f) Comparison of fatigue resistances as a function of cobalt content and strain history at $\Delta e_D^P = 0.00101$

FIGURE 12. (Concluded)

37918 SEM 35x

(a) Overview of surface

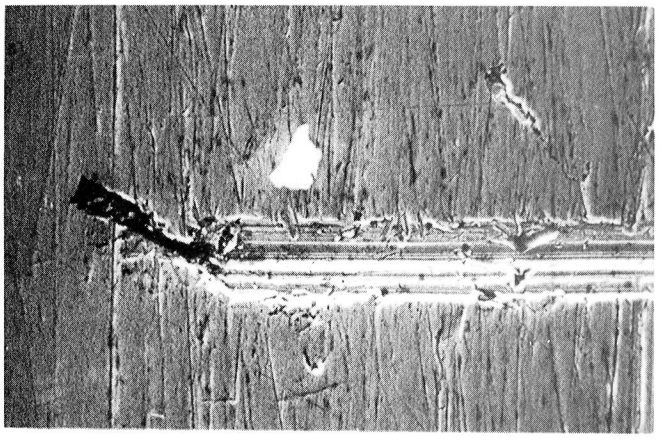

37917 SEM 400x

(b) Detail of one scar evident in part (a)

FIGURE 13. EXAMPLE OF SURFACE DEFECTS - SAMPLE D5-1884-9

Table 7. SPECIMENS RETURNED FOR REWORKING (1-18-83)

Specimen No.	Specimen No.
2-2-6 #2	D5-1886-7 #2
2-2-9 #3	D5-1886-7 #3
2-2-9 #4	D5-1886-7 #4
2-2-9 #5	D5-1886-9 #5
3-1-10 #2	D5-1885-3 #1
3-1-10 #3	D5-1885-6 #2
3-2-10 #4	D5-1885-6 #3
3-2-10 #5	D5-1885-11 #4
D5-1884-4 #1	D5-1885-11 #5
D5-1884-4 #2	
D5-1884-4 #3	
D5-1884-4 #5	

Fatigue resistance data for continuous cycling is presented in Figure 12 on coordinates of diametral plastic strain and cycles to separation. Data developed in this study, shown as open symbols, compare favorably with results available from a preliminary NASA-Lewis study, which are shown as solid symbols. Note that data for 12.8 percent cobalt content lie as a lower bound to results for other alloys and that the remainder of the data do not otherwise show any trends. Figure 12(b) presents these same data in terms of cycles to the first indication of cracking. Again, the data for 12.8 percent cobalt form a lower bound to the observed data. However, the remaining data now exhibit a pattern that shows the greatest resistance develops at 0.1 percent and 8.6 percent cobalt contents.

Figure 12(c) plots the ratio of first indication of cracking, R_o, to life separation, R_f, for the data presented in Figures 12(a) and (b). Observe that values of this ratio are not a function of plastic strain and that R_o/R_f ranges from about 0.1 to near unity. Now, for the same crack length e_D^P provides a reasonable measure of crack driving force. Also, it is reasonable to assume that the fracture toughness is nearly constant so that the crack growth period would also be constant for the same initial flaw size at constant e_D^P. Given the ordered dependence of R_o as a function of e_D^P, one can conclude that the differences in trends between parts (a) and (b) in Figure 12 develops because of different crack growth periods, which if toughness is a constant must be due to different iniitial flaw sizes. Clearly, randomly-sized flaws are present in these samples, to the extent that a number of samples were returned for retooling. For this reason, subsequent evaluation of the role of cobalt content and strain history are made in terms of R_o for this material. This includes the results developed for hold time cycling shown in Figure 12(d) which also show the scatter in R_o/R_f evident in the continuous cycling data.

Figure 12(e) which presents the hold time data compared to the scatter band for the continuous cycling results does not show any repeated pattern in the resistance as a function of hold time. The

results for the lower cobalt contents follow the pattern for the PM material. However, at higher cobalt contents this pattern breaks down, as evident in Figure 12(f) which crossplots resistances for a common strain: $e_D^P = 0.001$. Based on Figure 12(f) the optimum resistance appears to develop at low to intermediate cobalt contents. Possible explanations as to why low cobalt contents provide optimum resistance are numerous, as noted for the PM material. One probable explanation relates to the formation of crack-like features and brittle phases in the microstructure at higher cobalt contents. However, much more work well beyond the scope of this study is needed to explore the viability of this and other postulates that may be advanced to rationalize the observed trends.

Regarding deformation response, as with the PM material, a compressive mean develops with tension holds and a tensile mean develops with compression holds. Examples of this behavior are shown in Figure 14. But, as found with the PM material, while these trends are compatible with some of the trends in resistance (with due allowance for scatter), analysis including mean stress does not consolidate these data. Thus one may conclude that the history dependent fatigue resistance arises for reasons beyond the deformation behavior that develops under hold time cycling; perhaps because of combined effects of plasticity and creep damage. Support for this possibility follows from the intergranular-like nature of the initiation and growth process, as shown for example in Figure 15 for the case of a tensile hold.

DISCUSSION

The objective of this study was to empirically evaluate the influence of cobalt content on the high temperature creep fatigue crack initiation resistance of three nickel-based alloys. The objective was met by testing hourglass samples at a strain range chosen to produce about 10^4 cycles to failure. As noted in presenting the results, assessment of the influence of cobalt content was complicated by the influence of the failure criterion and the mode of data presentation. For example,

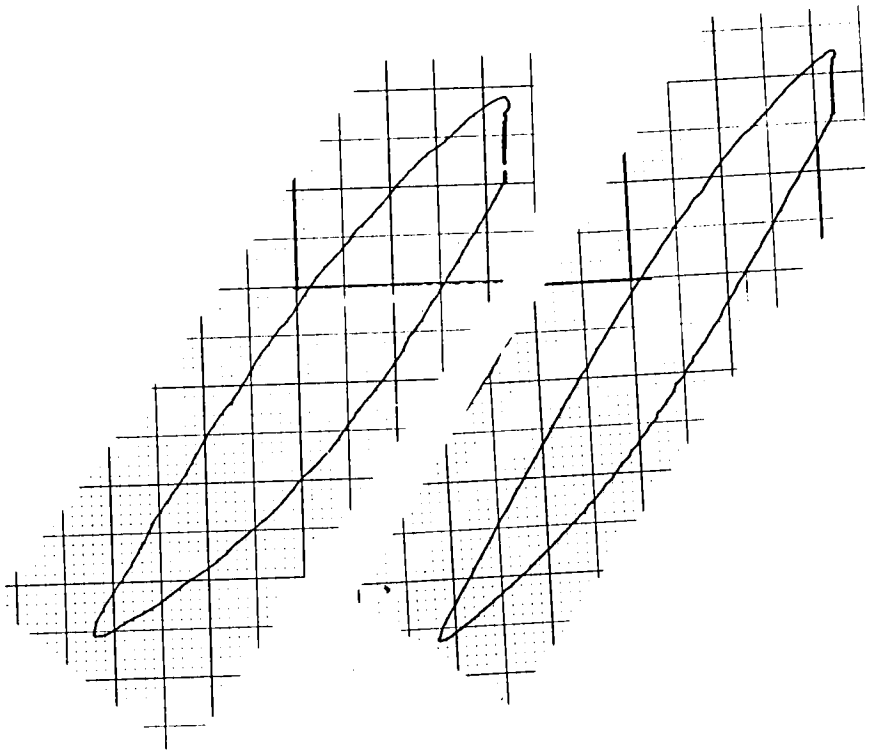

D5-1885-6-3;
1320 cycles

2-2-9-3;
1345 cycles

(a) Tension hold cycling

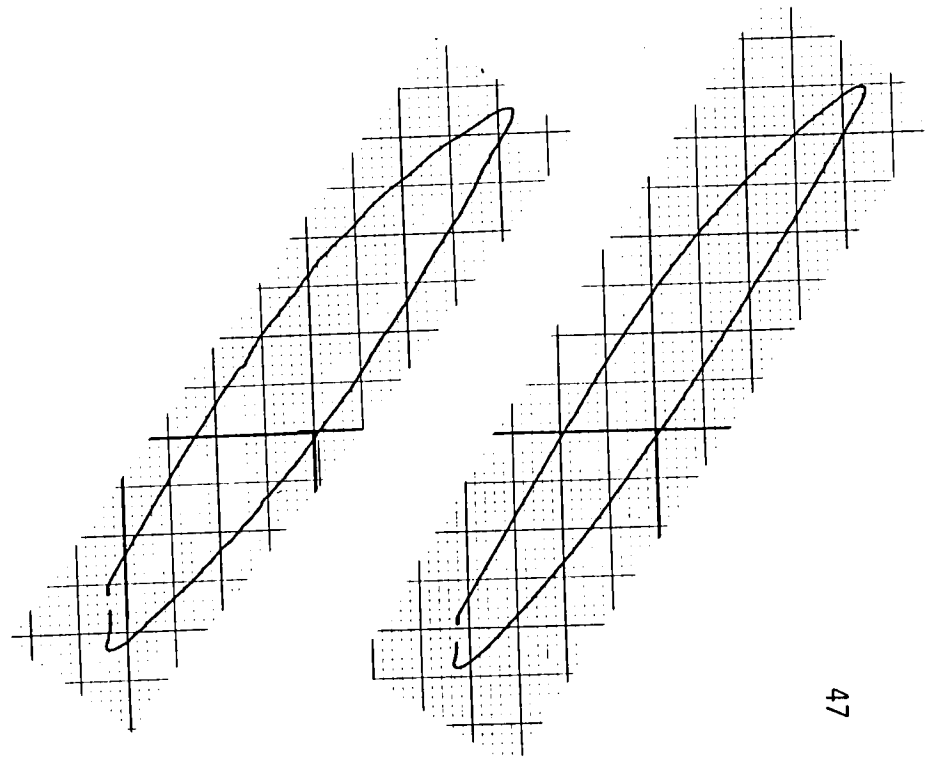

D5-1885-11-4;
143 cycles

3-2-10-4;
236 cycles

(b) Compression hold cycling

FIGURE 14. MEAN STRESSES DEVELOPED UNDER ASYMMETRIC HOLD TIME CYCLING AT 760 C

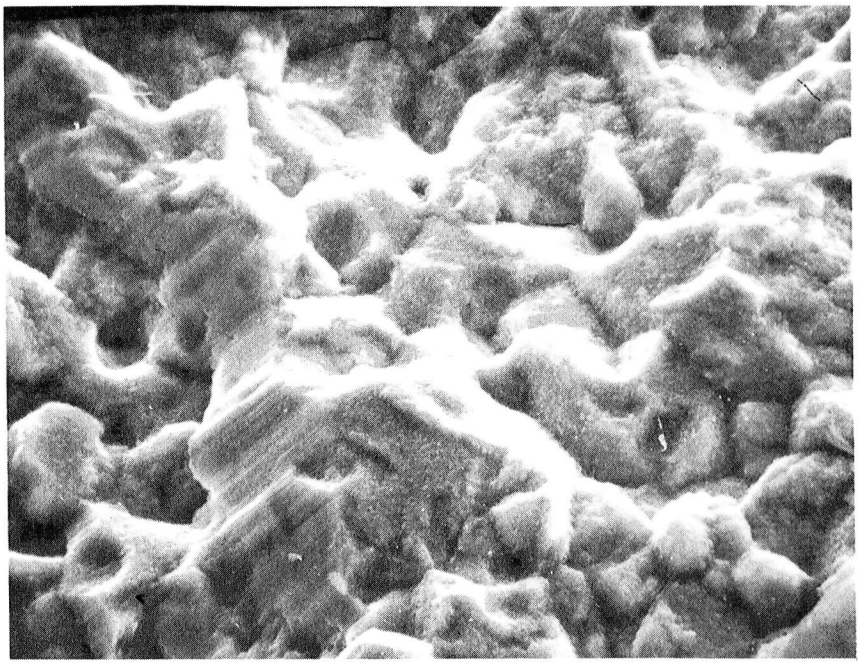

37922 SEM 3000x

FIGURE 15. EXAMPLE OF INTERGRANULAR LIKE FEATURES - SAMPLE 2-2-9-3 (SOME MECHANICAL DAMAGE ALSO EVIDENT)

early on, plastic strain was chosen rather than total strain as the mode for presentation to resolve differences in interpretation. This choice was supported on technical grounds related to the fundamental role of plastic strain in the fatigue damage process. But, the fact remains that total strain is a better criterion at longer lives, so that the choice made may be tenuous in some COSAM applications*. Similar problems develop interpreting data for situations where different fractions of N_o/N_f develop over the range of data being compared. This problem was noted as being particularly acute when the significance of cobalt to the crack initiation and growth resistances differs. Again the choice to use N_o rather than N_f may lead to conclusions that would be inappropriate for certain COSAM applications.

It follows from the above that the eventual application of a material in part controls what cobalt level would be optimal. Given the apparent sensitivity of thermal fatigue and cyclic oxidation resistance to cobalt content, it may be that the best comparitive elevated temperature resistance testing would involve thermal mechanical fatigue (TMF) cycling (perhaps with hold times) in an aggressive environment characteristic of fuel impurities or extreme operational conditions. Such tests, while more difficult to perform, may better define the service significance of cobalt content. But regardless of the specific test performed, it would be advisable to perform these tests over a broader range of lives. Such studies are relevant in that they would show "crossover" patterns in optimal cobalt content if the mechanisms controlling initiation and growth change with the increase cycle times. Finally, the viability of predictive methods for creep-fatigue or TMF analysis should be verified. This verification should focus on domains where plastic strains may be small thereby permitting the effect of hold-time induced mean stresses to continue throughout the life of components.

---

* It should be noted that similar confusion might develop if the results were compared in terms of axial versus longitudinal strain, depending on the ratio of e_D^p / e_D^e.

SUMMARY AND CONCLUSIONS

The results of this empirical study are summarized in Figures 6(e), 9(f), and 12(f). These data show that

- confusion in interpretation develops due to the mode of data presentation and the failure criterion
- the hold time history dependence of the resistance is as significant as the influence of cobalt content
- increased cobalt content does not produce increased creep-fatigue resistance on a one-to-one basis.

REFERENCES

1. COSAM Program Overview NASA TM-83006, 1982.

2. McGaw, M. A., Unpublished data - preliminary COSAM testing, April, 1982.

3. Anonymous, Aerospace Structural Metals Handbook, 1968.

4. INCO - High-Temperature High-Strength Nickel Base Alloys, 3rd Edition, 1977.

5. Lerch, B. A., "Microstructural Effects on the Room and Elevated Temperature Low Cycle Fatigue Behavior of Waspaloy", NASA CR-165497, 1982.

6. Cowles, B. A., Sims, D. L., and Warren, J. R., "Evaluation of the Cyclic Behavior of Aircraft Turbine Disk Alloys", NASA CR-159409.

7. Anonymous, MIL-HDBK-5 D, 1983.

8. Vitovec, F. H., and Lazan, B. T., "Fatigue, Creep and Rupture Properties of Heat Resistant Materials", WADC TR 56-181, 1956.

9. Swindeman, R. W., Unpublished results - private communication.

10. Jones, W. B., "Influence of Magneto-Mechanical Effect in Testing of Inductively Heated Ferritic Steel", Scripta Met, Sept., 1982, pp - .

APPENDIX A

MAGNETOMECHANICAL EFFECTS

APPENDIX A

MAGNETOMECHANICAL EFFECTS

It can be inferred from the literature that nickel-base materials may be subject to a magneto-mechanical effect[10]. That is mechanical cycling of specimens heated to a control thermocouple mounted outside the minimum test section will incur thermal cycling about a temperature other than that imposed. Magnetomechanical effects may change the apparent deformation response, including the elastic modulus, the extent depending on the shape of the specimen, the location of the thermocouple, physical constants of the material, and the nature of the loading/cycling.

Concern arose for a possible magnetomechanical effect when a loop tip hysteresis (e.g. Figure 8(b)) was noted in Waspaloy hold time tests. This behavior resulted in an increase in force at steady strain over the duration of the hold time, with unloading occurring from that point (see the example figure). Such behavior may occur in all such tests--however, it may go undetected if it is offset by a greater rate of relaxation!

Several experiments were performed to estimate the possible significance of the magnetomechanical effect in the present study. One sample of AF2-1DA designated number 89 by NASA and TAZ-8A designated number 9 by NASA were used in the absence of samples of Waspaloy or U 700. Their use is justified, however, because their heat transfer and Ni contents are similar to the materials investigated. Results of this preliminary study showed substantial temperature changes could be obtained as a function of the imposed strain. Consequently, selected histories comparable to these used in this study were among those imposed, and only these results are reported.

Results for the segment of the various loadings imposed that matched the histories of this study (obtained from TAZ-8A-9) indicated that the worst temperature shift from steady state is only 3 C. The maximum temperature cycle is observed to be 5 C (-2 to +3) from steady state. These numbers suggest that the test temperature desired has been reasonably achieved, such that the data may be reported for the

nominal temperature sought in this study. Strains associated with the 5 C cycle are about 7×10^{-5}. Stresses (which have been calculated with a modulus which in the absence of detailed results has been assumed independent of the magneto-mechanical effect) produces about a 14 MPa stress increase at constant strain. This shift is somewhat less than observed--but this discrepancy may be tentatively attributed to the assumed modulus.

The above calculations indicate that the stress and plastic strain developed in these tests are slightly less than would be expected at the imposed total diametral strain. The fatigue resistance trends reported, therefore, are expected to fall only slightly below those in other studies wherein the magneto-mechanical effect did not develop. However, the relative resistances will not be affected meaning that the objective of this study is not in jeopardy as a result of the effect.